united nations
educational, scientific
and cultural
organization

international atomic
energy agency

the
abdus salam
international centre for theoretical physics

SMR: 1343/4

EU ADVANCED COURSE IN COMPUTATIONAL NEUROSCIENCE

An IBRO Neuroscience School

(30 July - 24 August 2001)

"Auditory Systems"

presented by:

Christoph SCHREINER
University of California
Coleman Laboratory
513 Parnassus Avenue
San Francisco, CA94143-0732
U.S.A.

Auditory System

Reviews:

Zigmond, Bloom, Landis, Roberts, Squire Fundamental Neuroscience (Academic Press, San Diego, 1999) Chapter 27, p791-820.

A.J. Hudspeth (1997) How Hearing Happens. Neuron 19:947-950.

Summary/Text Books:

B.C.J. Moore: An Introduction to the Psychology of Hearing. 4th Edition. Academic Press 1997.

Bregman, Albert S., Auditory Scene Analysis: The Perceptual Organization of sound. Cambridge, Massachusetts: The MIT Press, 1990 (hardcover)/1994 (paperback).

C.D. Geisler: From Sound to Synapse. Oxford Press, 1998.

P. Dallos, A.N. Popper, R.R. Fay: The Cochlea. Springer Handbook of Auditory Research Vol. 8, Springer, 1996.

Ehret, G., Romand, R. The Cnetral Auditory System. Oxford University Press, 1997.

D.B. Webster, A.N. Popper, R.R. Fay: The Mammalian Auditory Pathway: Neuroanatomy. Springer Handbook of Auditory Research Vol. 1, Springer, 1991.

A.N. Popper, R.R. Fay: The Mammalian Auditory Pathway: Neurophysiology. Springer Handbook of Auditory Research Vol. 2, Springer, 1991.

H.L. Hawkins, T.A. McMullen, A.N. Popper, R.R. Fay: Auditory Computation. Springer Handbook of Auditory Research Vol. 6, Springer, 1995.

Physical Attributes	Psychophysical Attributes
Frequency	Pitch
Amplitude	Loudness
Phase	- - - -
Amplitude modulation	Periodicity Pitch Roughness
Spectral Composition	Timbre Sound localization
Binaural differences Intensity, timing	Sound localization

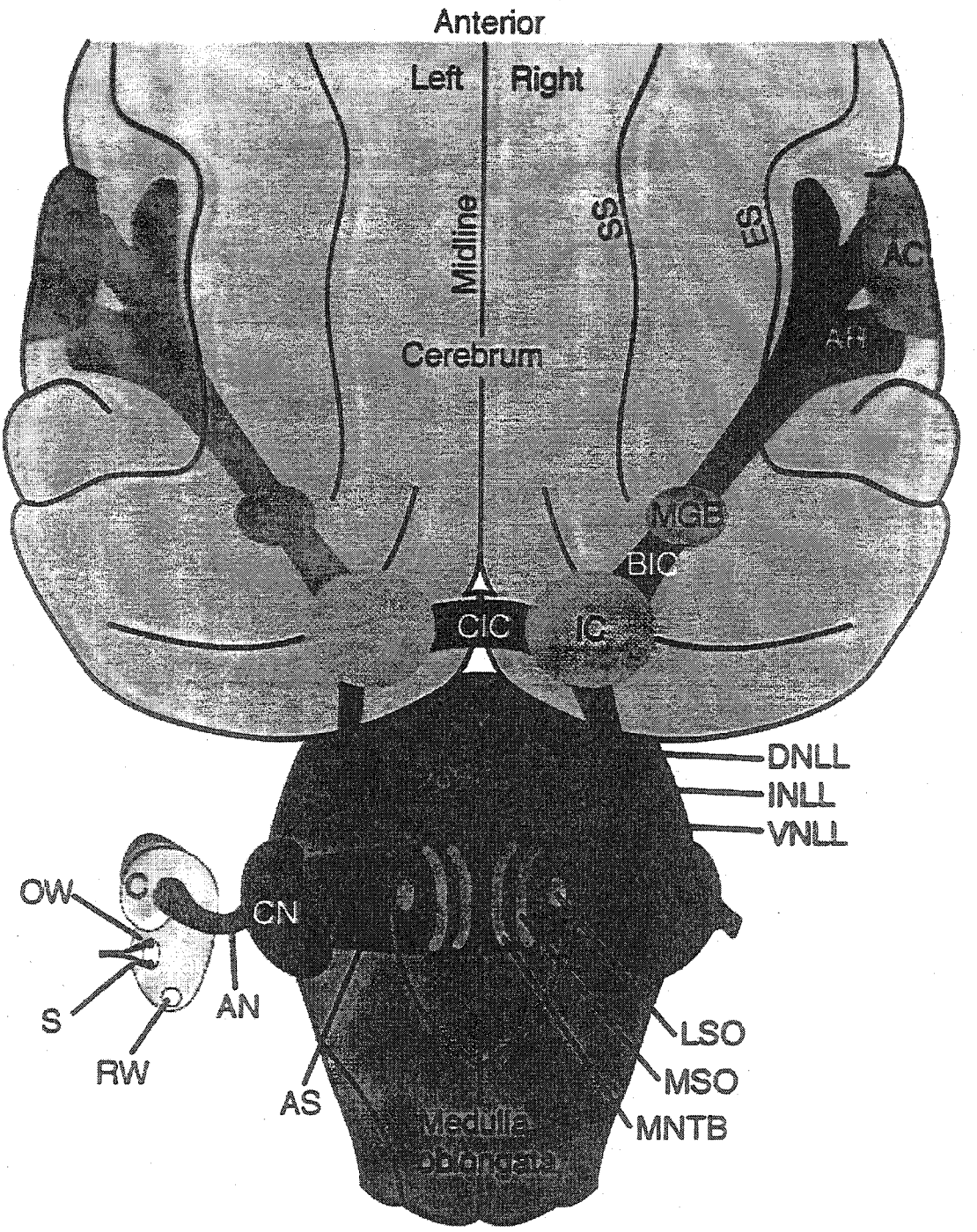

FIG 27.2

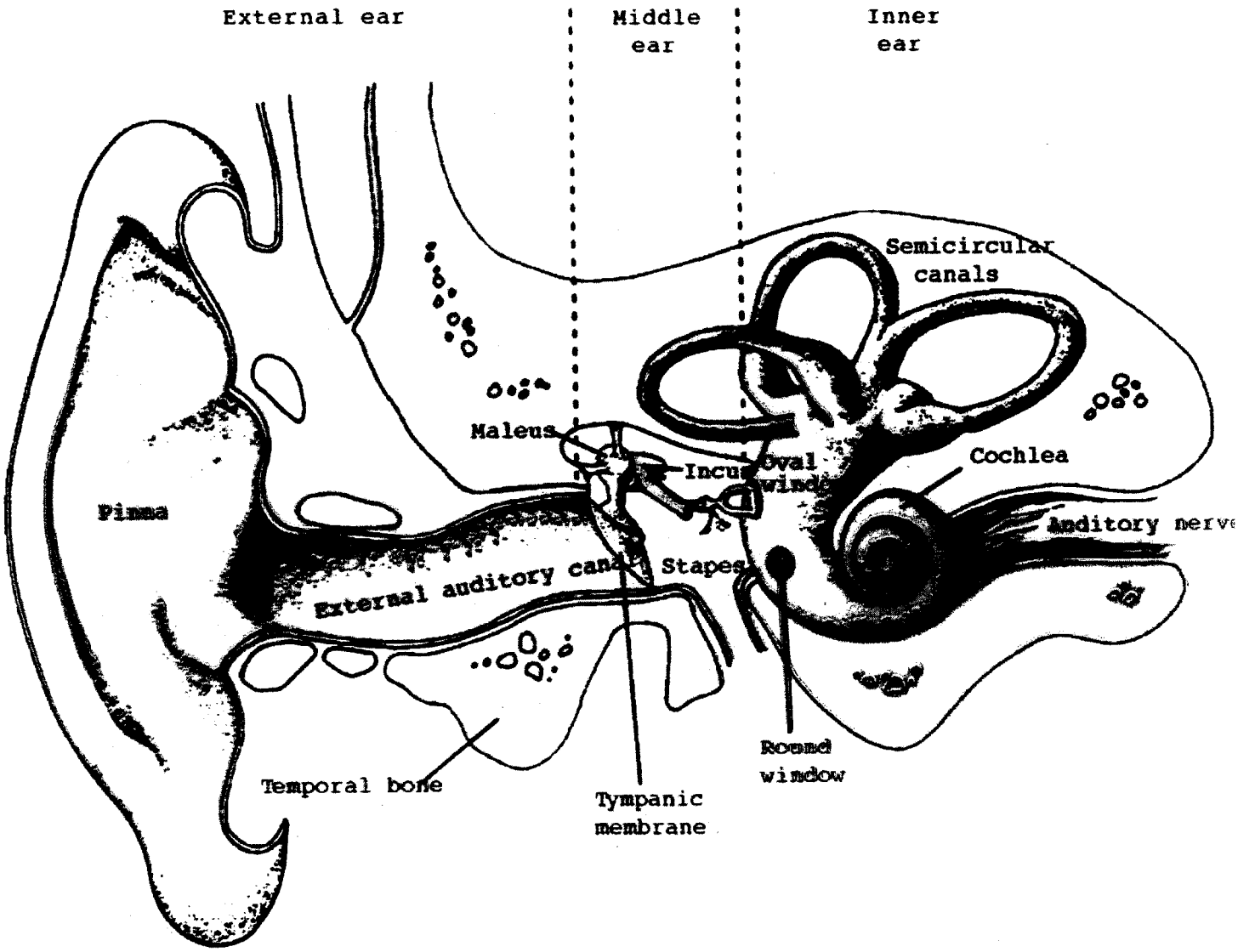

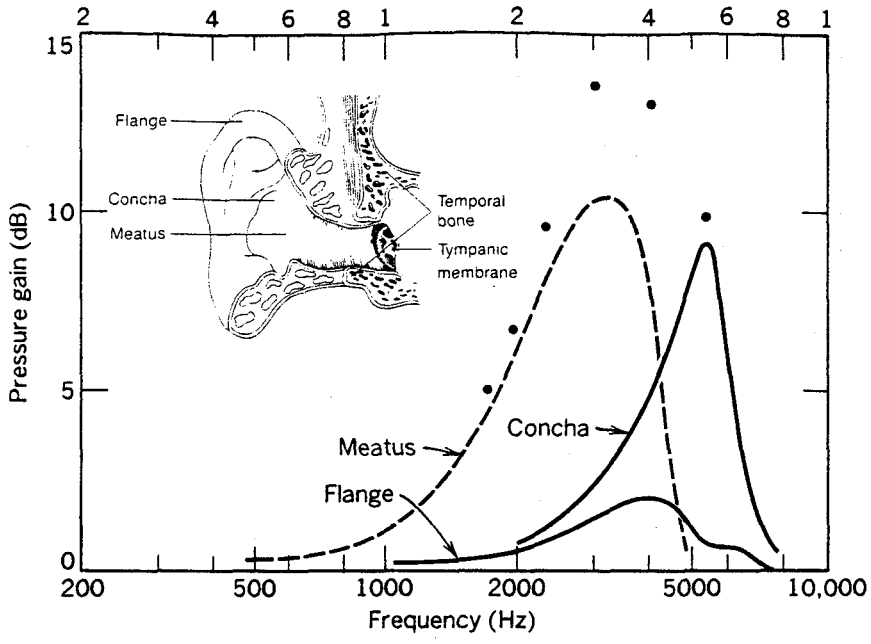

Fig. 4.2. The insert shows the pinna in the coronal view, with the flange and concha identified. The solid lines show the acoustic pressure gain in decibels as a function of the stimulus frequency that results from each of these structures. The dashed line shows the gain that results from resonance in the external meatus. The solid unconnected circles show the total acoustic gain produced by the external ear. Sound source at 45° azimuth. Data from Shaw (25, p. 468).

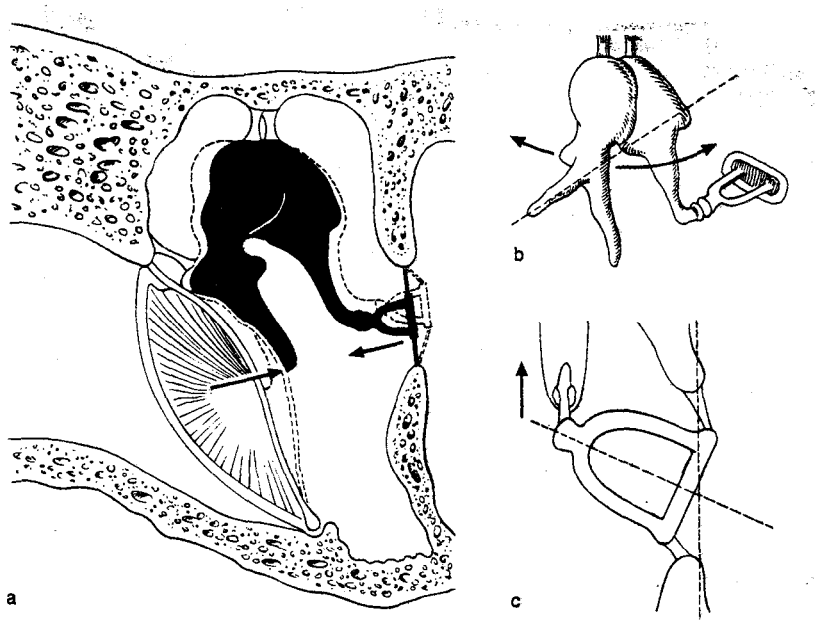

Abb. 1.**68** Hypothesen zum Bewegungsablauf der Gehörknöchelchen.

a Tonische Bewegungen bei statischem Druck auf das Trommelfell (Verschiebung der Knochen = rotbraun); die Pfeile geben die Bewegungsrichtung an.

b Dynamische Hammer-Amboß-Drehbewegung (gestrichelte Linie: Rotationsachse).

c Möglichkeit der Kippbewegung des Steigbügels (nach Rauber u. Kopsch [508]).

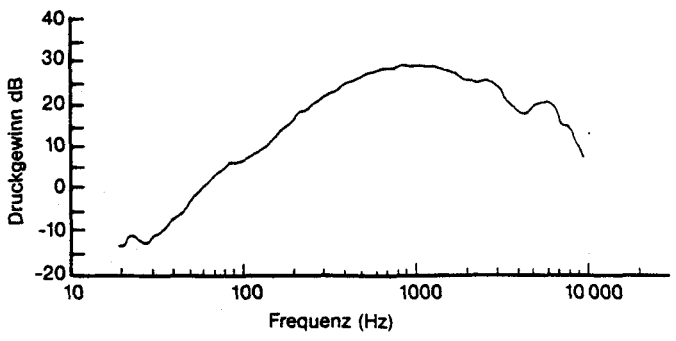

Abb. 1.**74** Die Übertragungsfunktion des Mittelohres: Darstellung des Druckgewinns in der Kochlea (Scala vestibuli, basale Windung) im Vergleich zum Trommelfell, in Abhängigkeit von der Frequenz (nach Nedzelnitsky [419]).

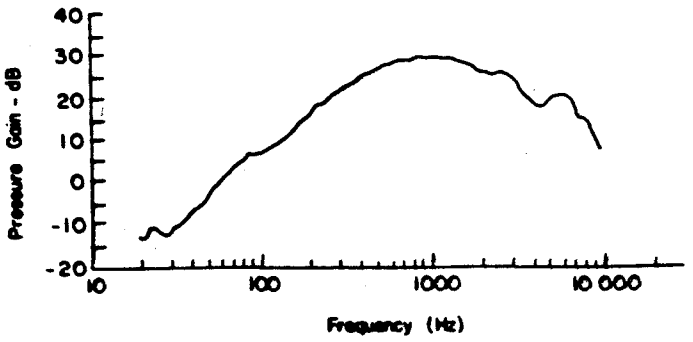
Pressure Gain - dB
40
30
20
10
0
-10
-20
10
100
1000
10 000
Frequency (Hz)

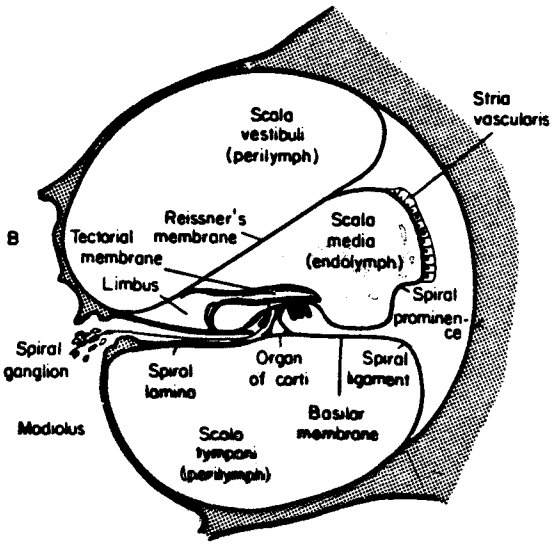
Stria vascularis
Scala vestibuli (perilymph)
B
Tectorial membrane
Reissner's membrane
Scala media (endolymph)
Limbus
Spiral prominence
Spiral ganglion
Spiral lamina
Organ of corti
Spiral ligament
Basilar membrane
Modiolus
Scala tympani (perilymph)

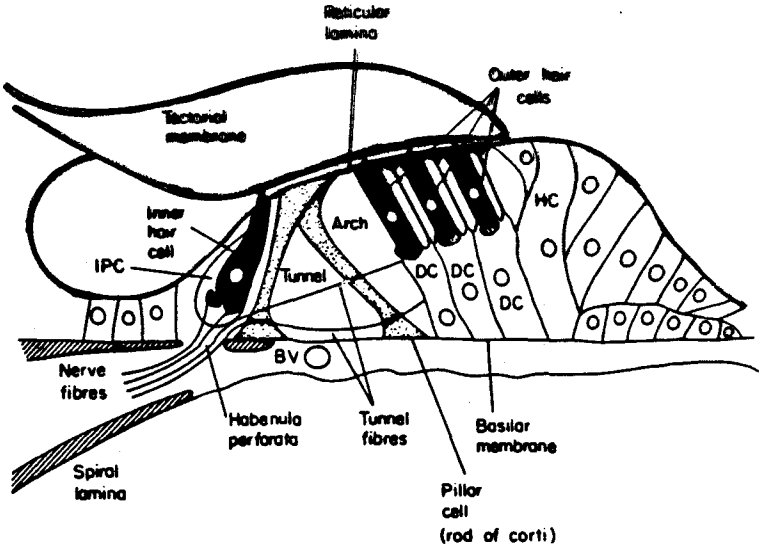
Reticular lamina
Outer hair cells
Tectorial membrane
Inner hair cell
IPC
Arch
Tunnel
DC
DC
DC
HC
BV
Nerve fibres
Habenula perforata
Tunnel fibres
Basilar membrane
Spiral lamina
Pillar cell (rod of corti)

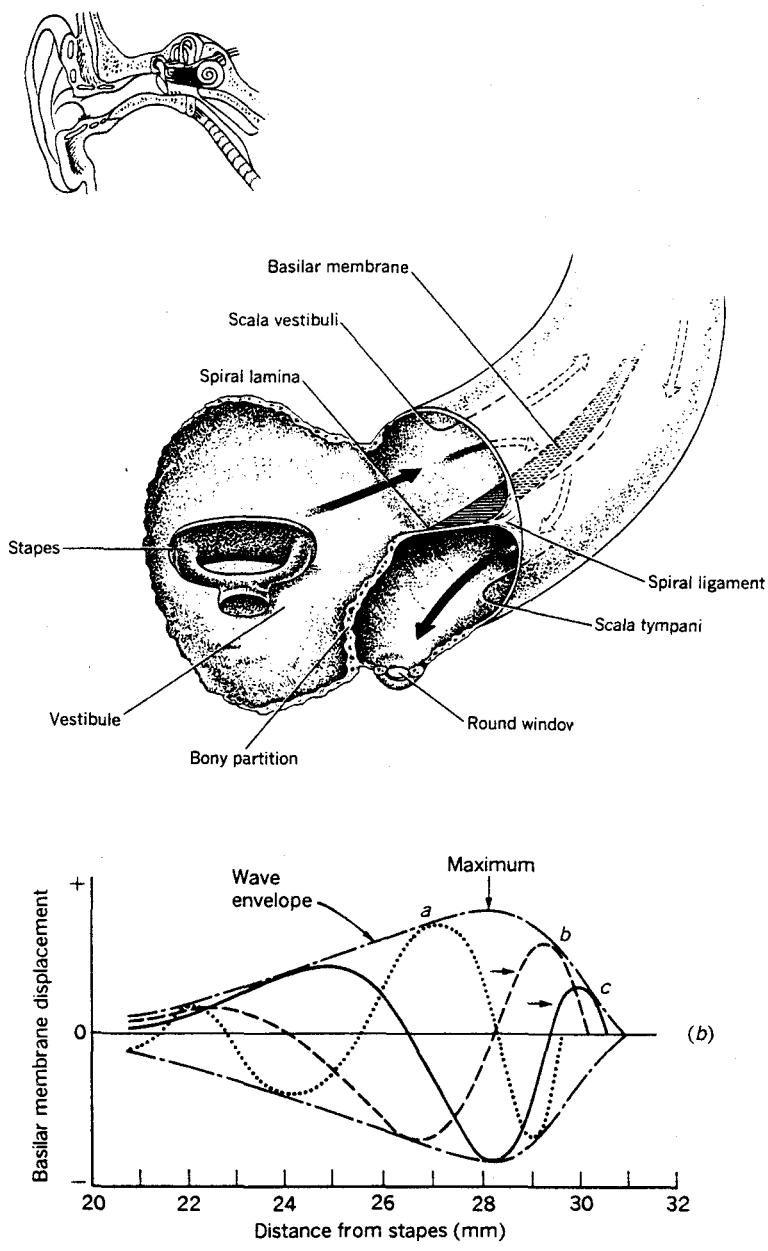

Fig. 6.1. (*a*) Schematic representation of the cochlea with the vestibule cut away. The arrows show the effects of a compressional sound wave produced by medial displacement of the stapes. (*b*) Example of the position of a portion of the basilar membrane in three successive instants (dotted, dashed, and solid lines) during sinusoidal stimulation (200 Hz) by a mechanical vibrator. After Békésy (3, p. 462).

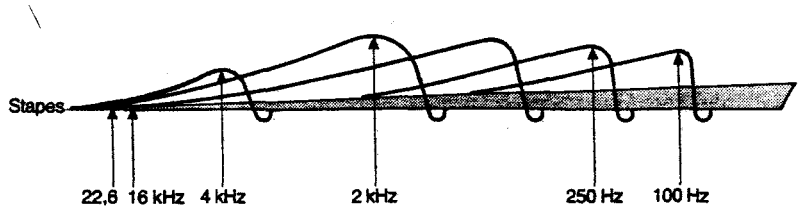

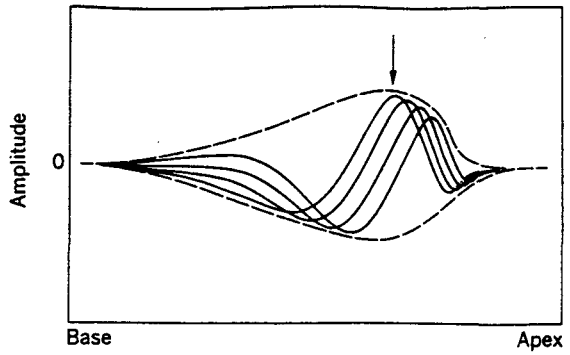

Fig. 6.5. The position of the basilar membrane at close successive intervals during sinusoidal stimulation to illustrate a traveling wave. The dashed line is the envelope of the wave, and the arrow denotes the place of maximum membrane displacement. After Békésy (3, p. 499).

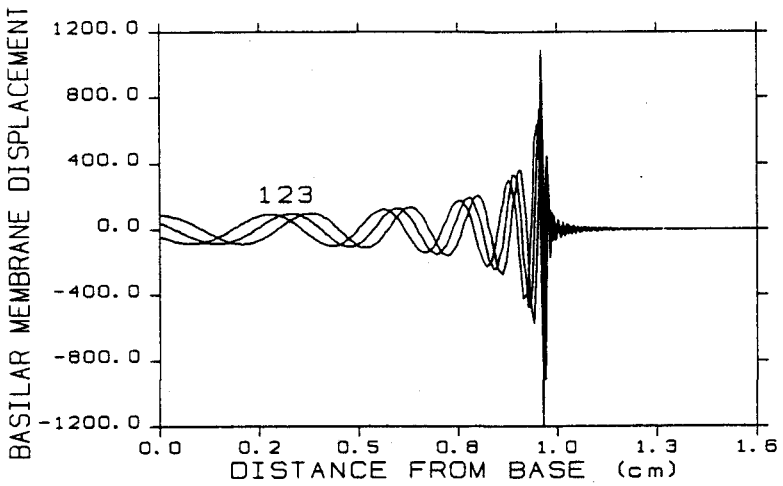

FIG. 1. Computer simulation of basilar membrane displacement for three points in time (numbered successively), illustrating the traveling wave (Simulation courtesy of Dr. A. E. Hubbard)

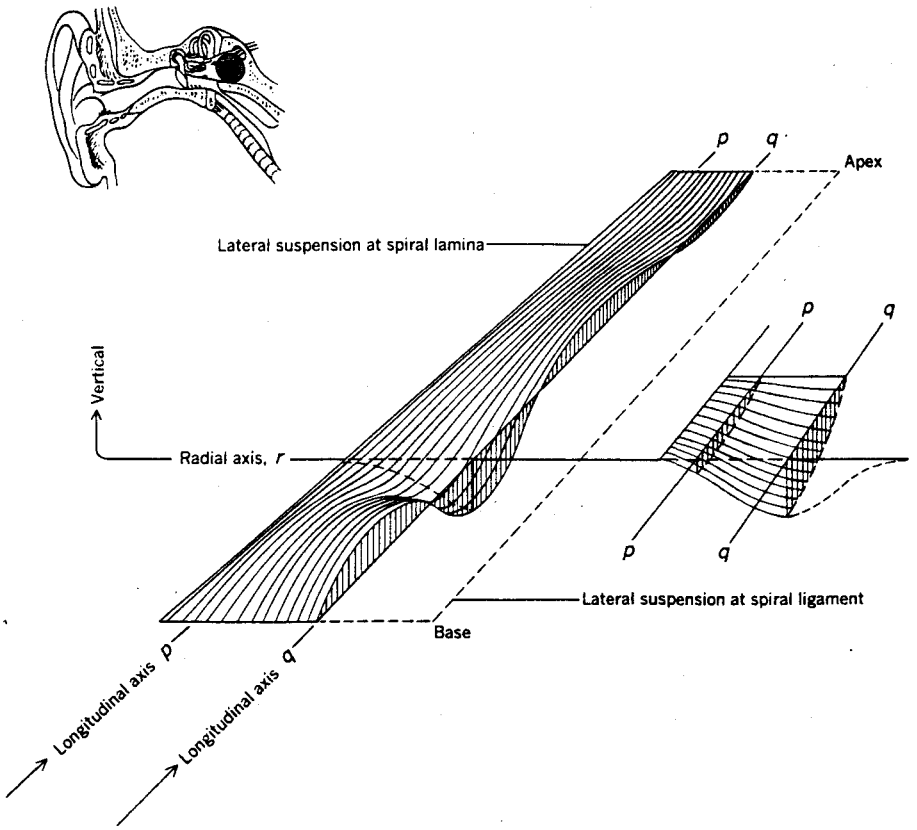

Fig. 6.9. Schematic drawing of an instantaneous waveform of the basilar membrane in longitudinal and transverse cross sections.

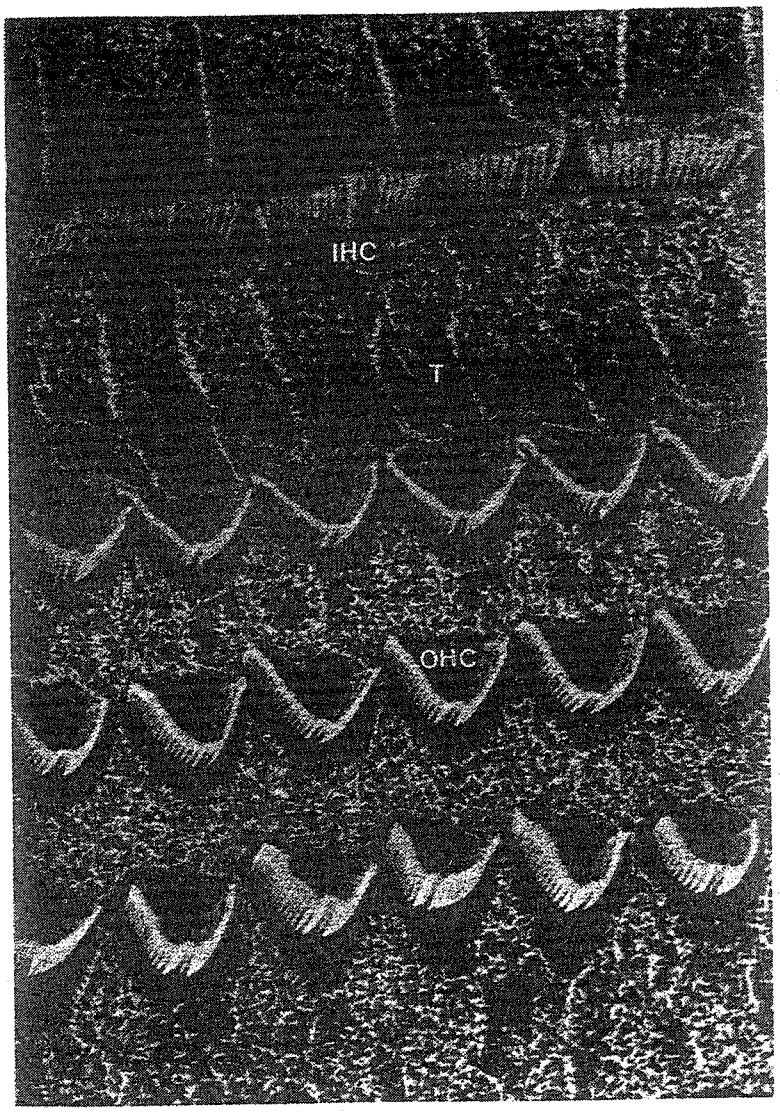

FIGURE 2.5 Comparison of the stereocilia on the apical surface of the inner (IHC) and outer (OHC) hair cells. The one row of IHCs and the three rows of OHCs are separated by the tunnel (T) composed of inner and outer pillar cells. (Scanning electron micrographs from guinea pig cochlea provided by Dr. G. Reiss, University of Hanover, Germany. From Reiss © 1992, reprinted by permission of John Wiley and Sons, Inc.)

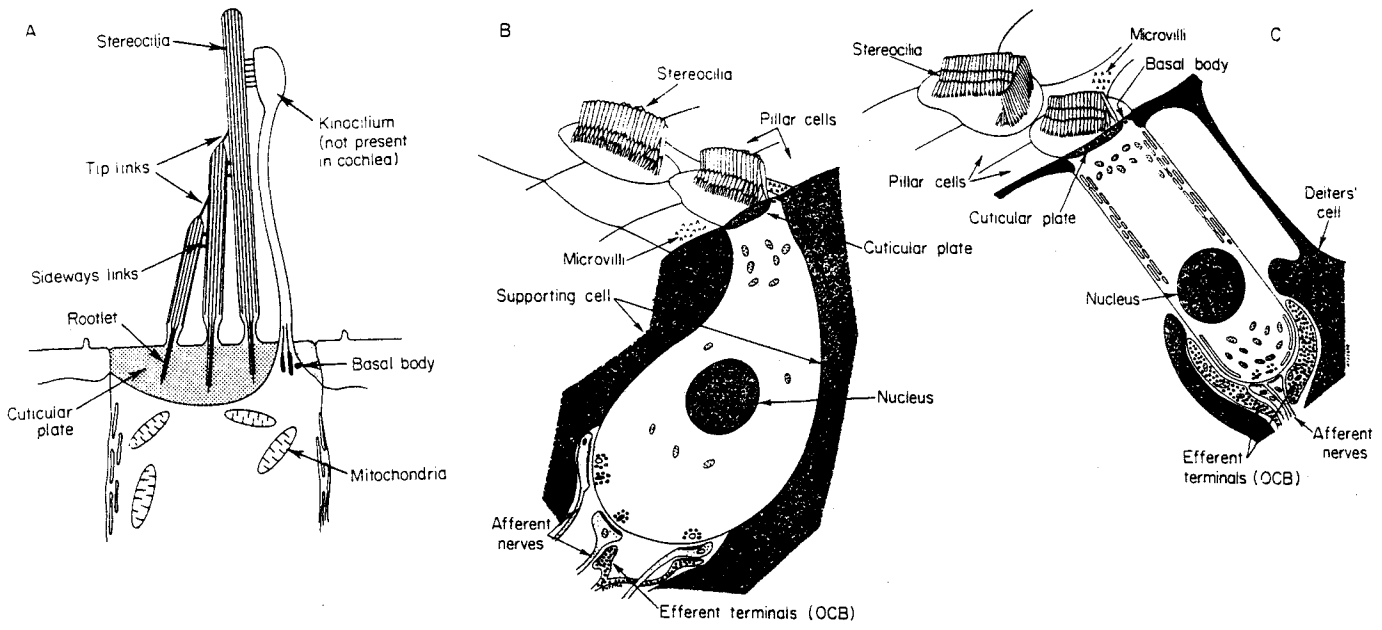

Fig. 3.5 (A) The common structures on the apical portion of acousticolateral hair cells include rows of stereocilia which are graded in height and joined by cross-links. The tip links may be involved in transduction, opening the transducer channels. The kinocilium is not present in the mature cochlea, although it is present in vestibular cells. (B) and (C) Inner hair cells are shaped like a flask (B), and outer cells are shaped like a cylinder (C). OCB, olivocochlear bundle. © J.O. Pickles 1987.

information from the cochlea to the brainstem. On the presynaptic membrane, the synapse is often marked by small dense synaptic bars or invaginations at right angles to the cell wall, or by rounded synaptic bodies, together with a few vesicles (Ades and Engström, 1974).

Outer hair cells are approximately 25 μm long in the basal turn and 45 μm long in the apical turn, and 6–7 μm in diameter (chinchilla: Smith, 1968). They have a cylindrical shape. The nucleus is located basally (Fig. 3.5C). The mitochondria are primarily situated at the base below the nucleus, and at the apex below the cuticular plate. The afferent terminals are faced with short synaptic bars, but not round synaptic bodies (Ades and Engström, 1974).

In both types of hair cell the row of tallest stereocilia and the gap in the cuticular plate are situated on the side of the hair cell furthest away from the modiolus, and the row of shortest stereocilia are situated nearest to the modiolus.

3. The Innervation of the Organ of Corti

The cochlea is innervated by about 50,000 sensory neurones in the cat, and about 30,000 in man (Schuknecht, 1960; Harrison and Howe, 1974a). There are also about 1800 "efferent" or centrifugal neurones, by means of which

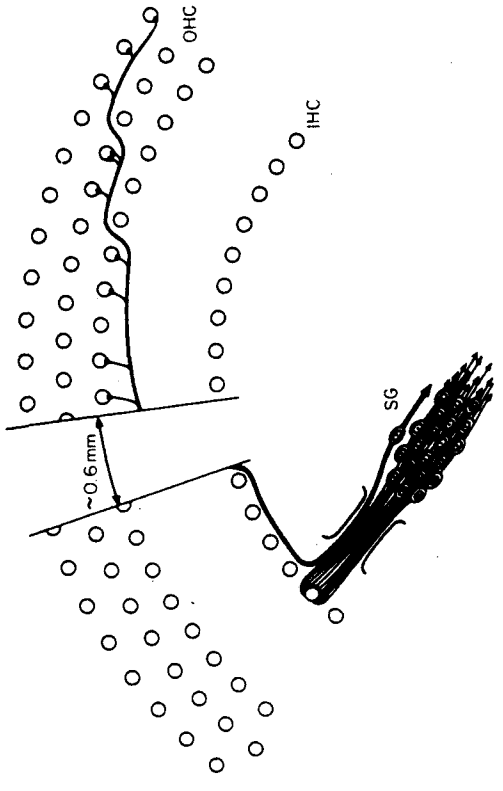

Fig. 3.6 The great majority of auditory nerve fibres (type I fibres) connect with inner hair cells. A few fibres (type II) pass to outer hair cells, after running basally for about 0.6 mm. IHC, Inner hair cells; OHC, Outer hair cells; SG, spiral ganglion. From Spoendlin (1978, Fig 8).

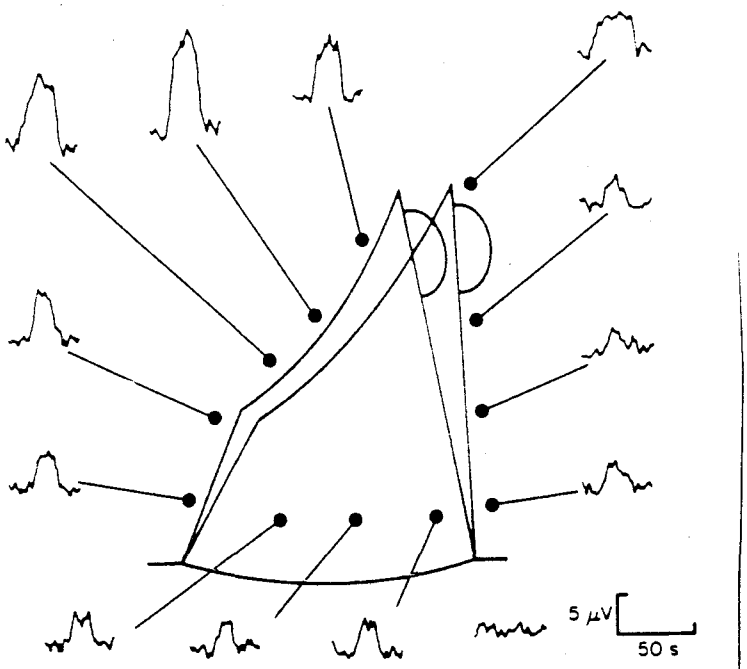
5 μV
50 s

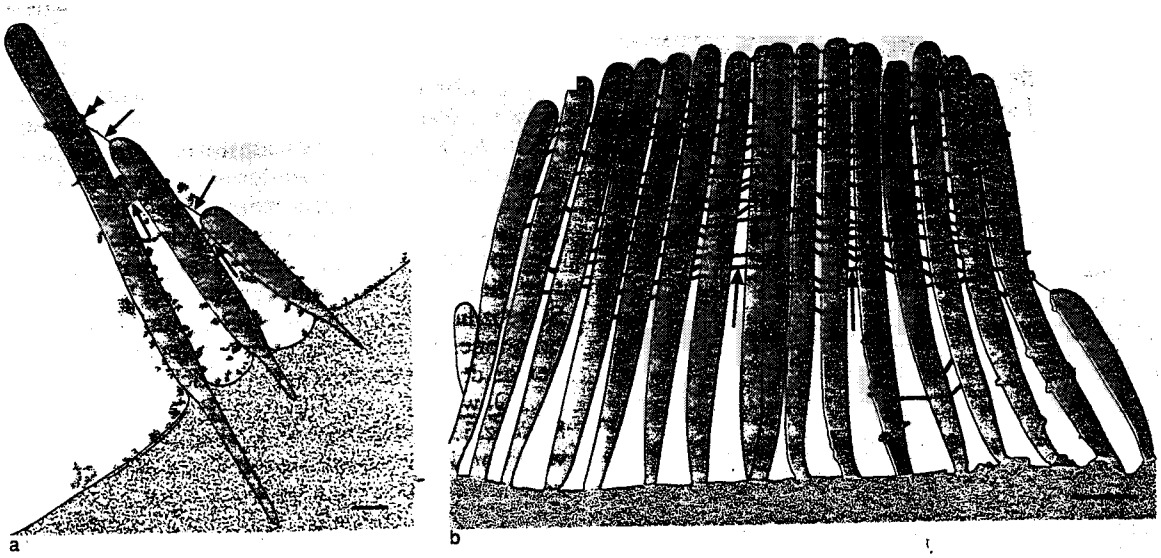
a
b

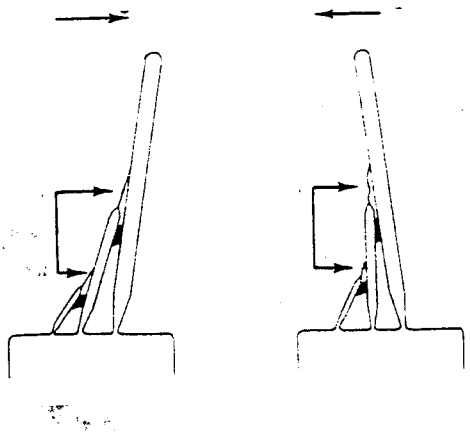

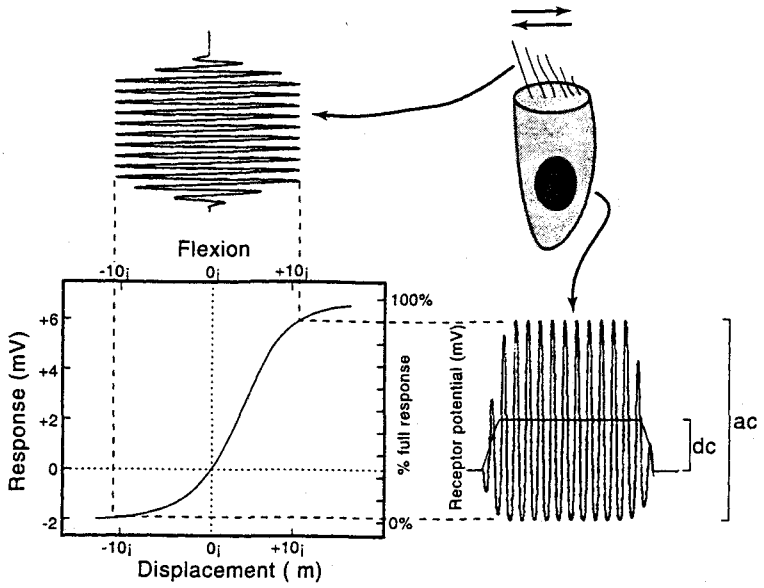

FIGURE 24.35 Sigmoidal input–output function of hair cell. Symmetrical sinusoidal displacement of stereocilia produces ac and dc receptor potential components. From: Hudspeth, A. J. and Corey, D. P. (1977). Sensitivity, polarity and conductance change in the response of vertebrate hair cells to controlled mechanical stimuli. *Proc. Natl. Acad. Sci. U.S.A.* **74**: 2047–2411.

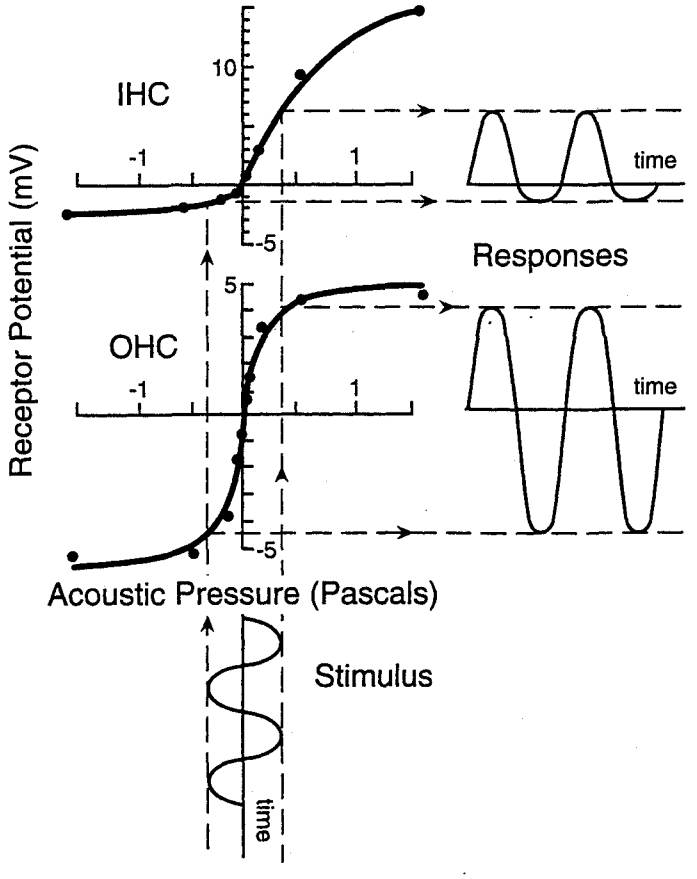

Figure 8.3. Generation of receptor potentials in an inner hair cell (IHC, top panel) and an outer hair cell (OHC, middle panel), with tonal excitation of about 84 dB SPL at low frequencies. The acoustic stimulus (bottom trace) changes the transmembrane potential according to each hair cell's input–output curve (left) resulting in the respective receptor potentials (right). (The input–output curves were obtained from Russell et al., 1986, with permission*.)

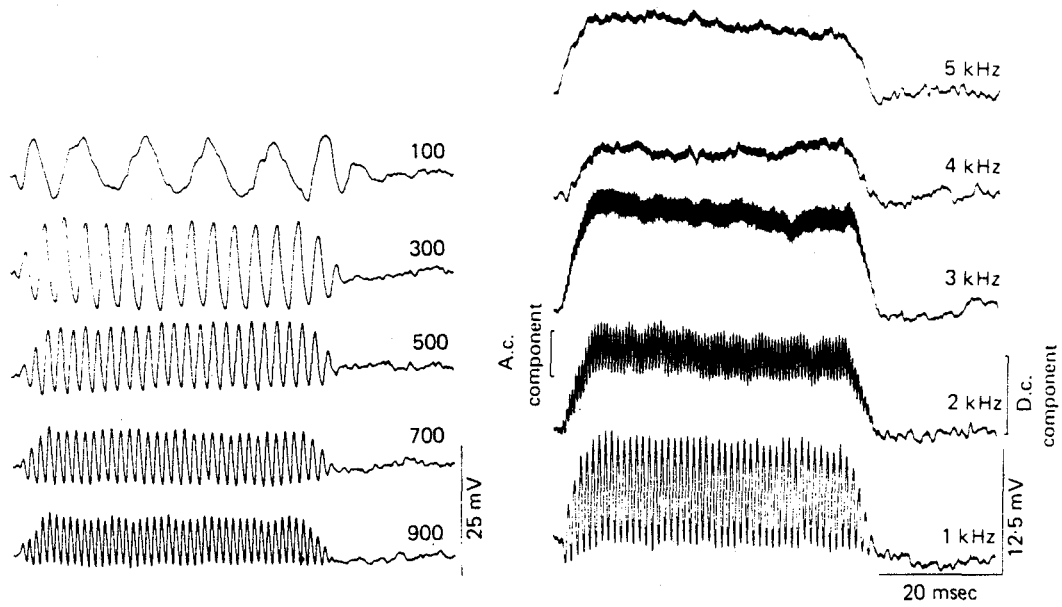

FIG. 3. Intracellular receptor potentials recorded from a guinea pig inner hair cell with a CF of approximately 20 kHz. The parameter of each tracing gives the stimulus frequency, and in each case the sound pressure level was held constant at 80 dB relative to 20 Pa. Notice that relative to the dc component the ac component is reduced as frequency is increased and the dc component dominates the response above 1 kHz. (From Russell and Sellick, ref. 121, with permission.)

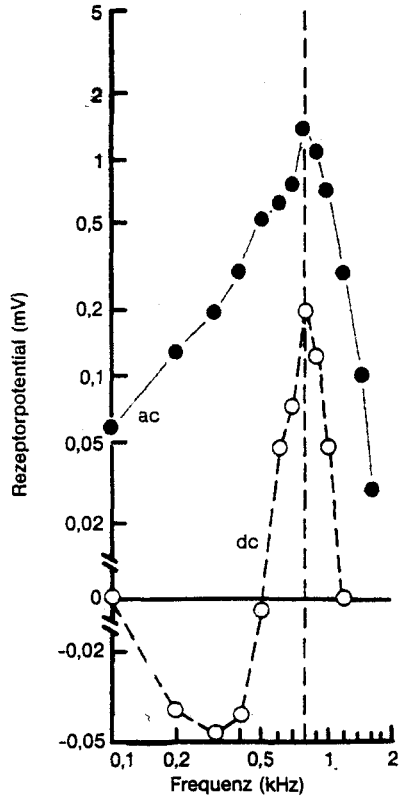

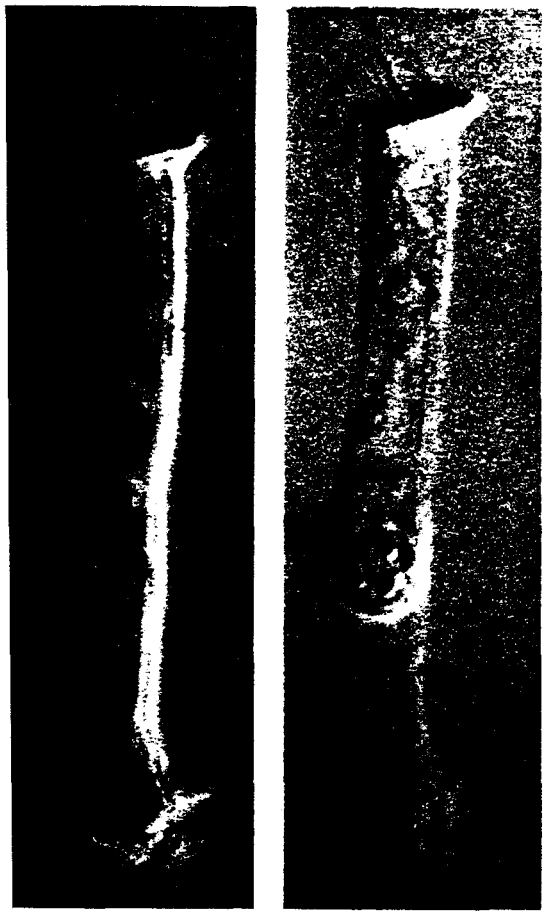


d
e

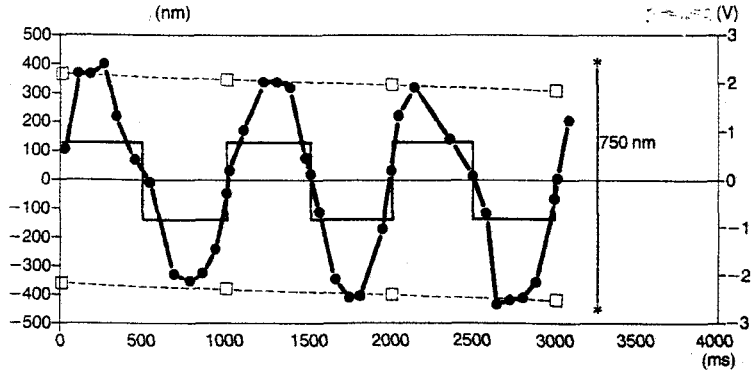
(nm)
(V)
500
400
300
200
100
0
−100
−200
−300
−400
−500
3
2
1
0
−1
−2
−3
750 nm
0
500
1000
1500
2000
2500
3000
3500
4000
(ms)

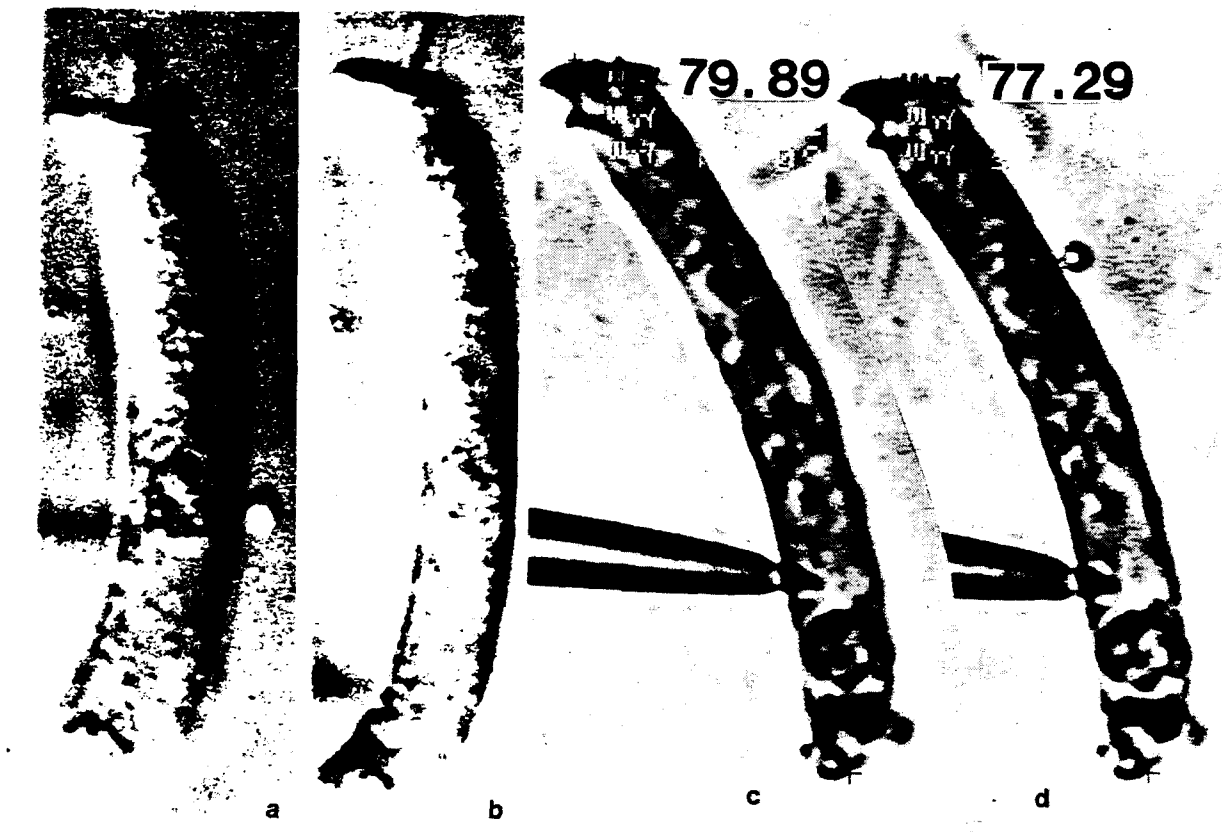
79.89
77.29
a
b
c
d

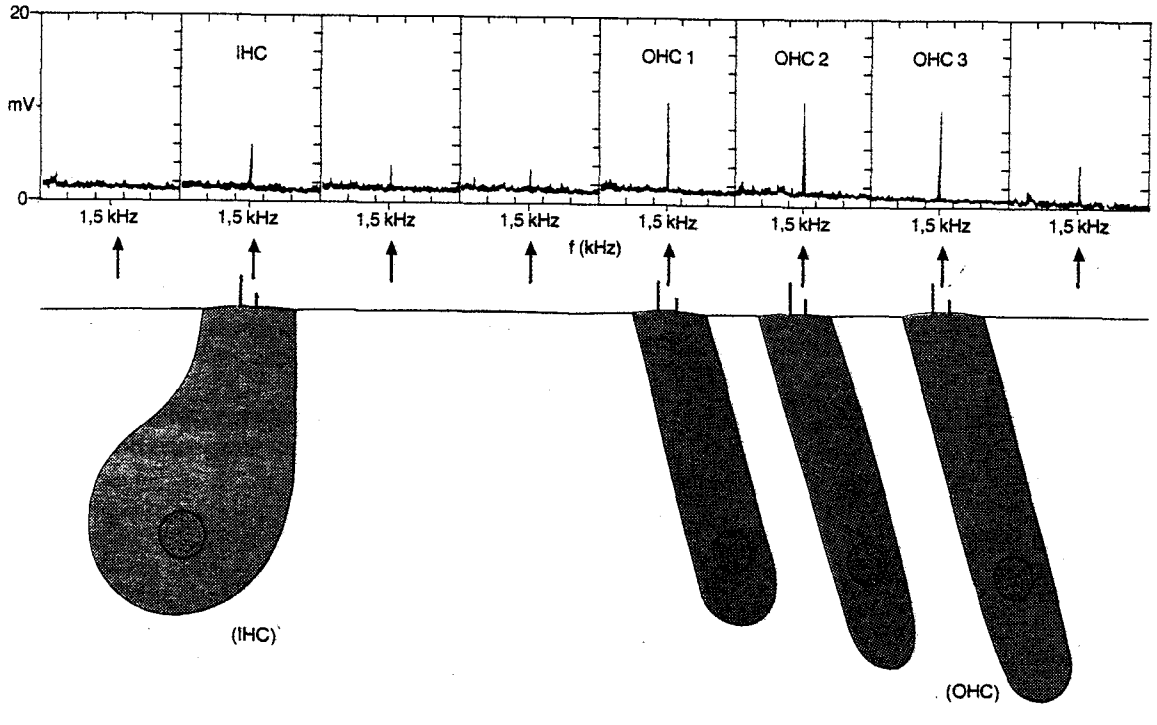
20
mV
0
IHC
OHC 1
OHC 2
OHC 3
1,5 kHz
1,5 kHz
1,5 kHz
1,5 kHz
1,5 kHz
1,5 kHz
1,5 kHz
1,5 kHz
f (kHz)
(IHC)
(OHC)

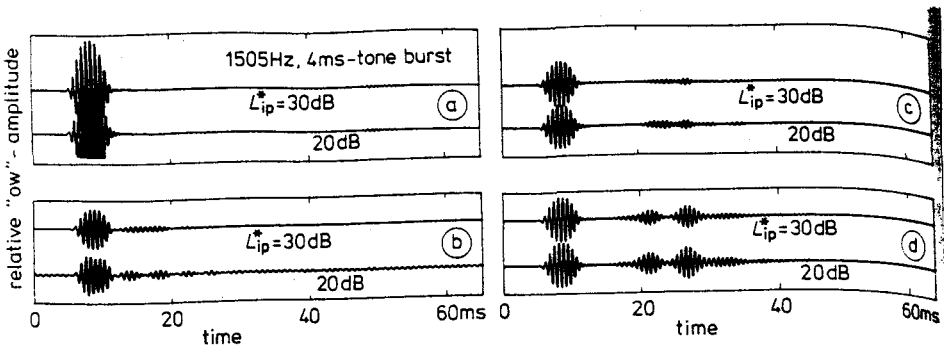

FIGURE 4: "DEOAEs" in the model, i.e. time functions of "oval window" - voltage with normalized amplitude as a response to a 1505-Hz tone burst of 4-ms duration and 2-ms Gaussian rise and fall time. Parameters as in Fig.3.

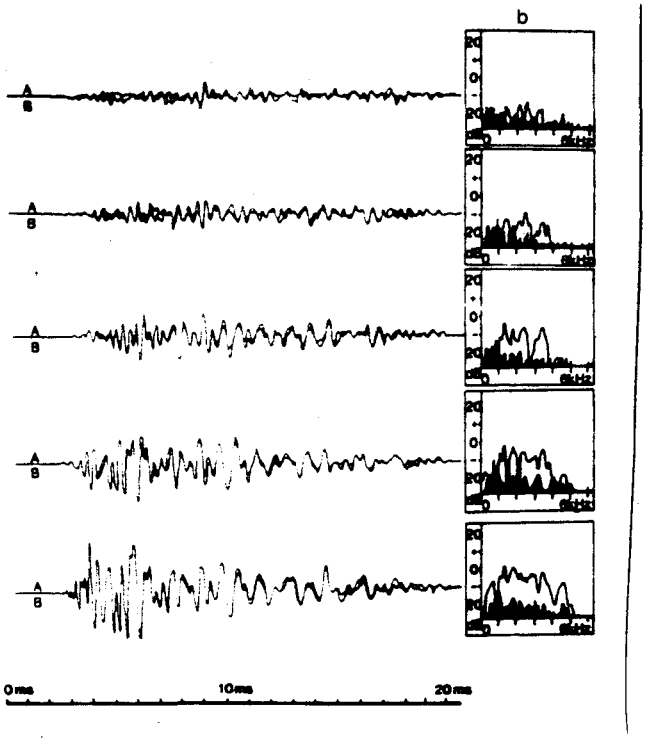

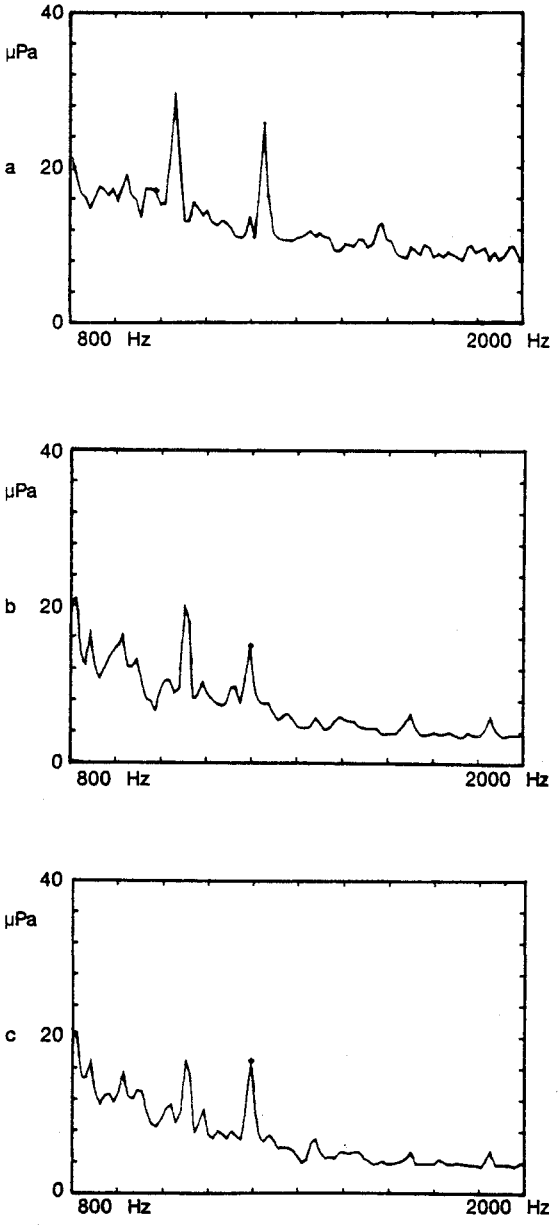

Abb. 1.93 Leistungsspektren von spontanen otoakustischen Emissionen eines Menschen. Gezeigt ist der im Gehörgang gemessene Schalldruck verschiedener emittierter Frequenzen nach Fouriertransformation. Sowohl auf dem rechten Ohr (**a**) als auch auf dem linken Ohr (**b**) konnten je 2 Emissionen gemessen werden, (**c**) gibt die konstanten Emissionen des rechten Ohres einige Tage später wieder (nach Plinkert u. Mitarb. [487]).

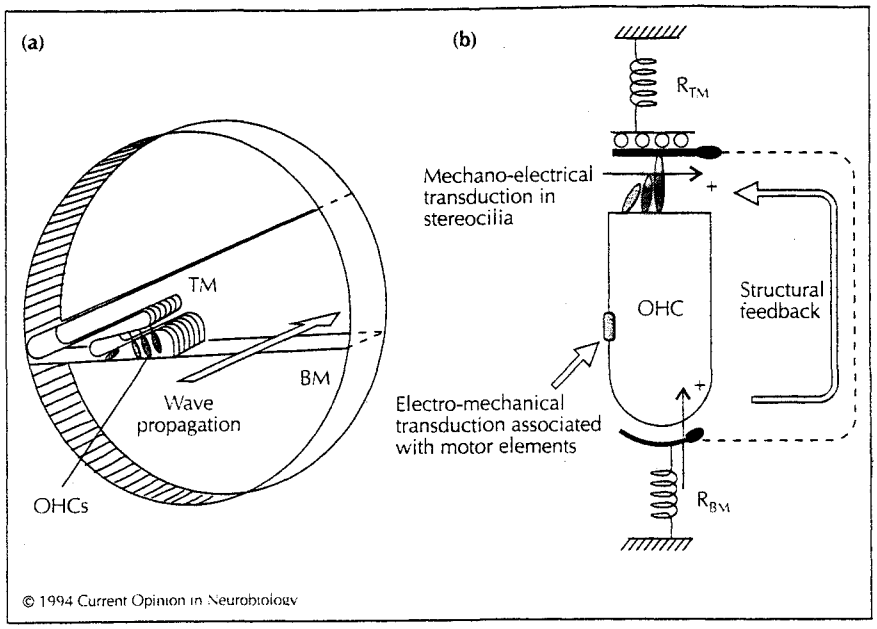

Fig. 2. The OHC building block. **(a)** Each OHC in the organ of Corti is coupled into the cochlear partition as part of a feedback loop involving both the (forward) mechano-electrical transducer at the stereocilia and the (reverse) electromechanical transducer step in the BM [2,6•,7]. **(b)** Deflection of the stereocilia elicits a change in membrane potential, which generates an axial cellular force from the motor (element only shown). The force acts against many mechanical structures. These include the spring elements R_{BM} and R_{TM} associated with the BM and the tectorial membrane, TM, respectively.

Sensory systems

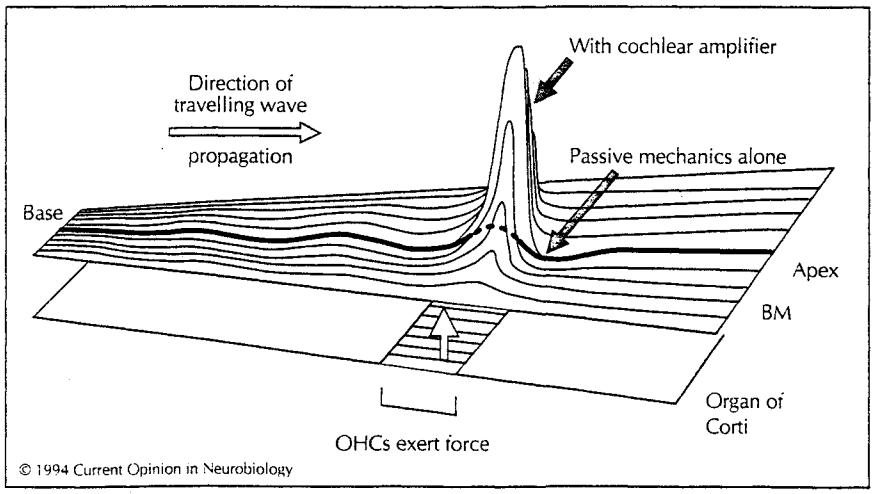

Fig. 1. Wave motion in the cochlea. Sound entering the cochlea sets up a travelling wave that propagates along the BM from the stapes at the base. The motion at the peak is enhanced, up to a hundred times, by the effects of cochlear amplification; the maximum excursion of the amplified peak is about 50 nm [5]. The position where about 200 OHCs in the organ of Corti exert force is shown [9].

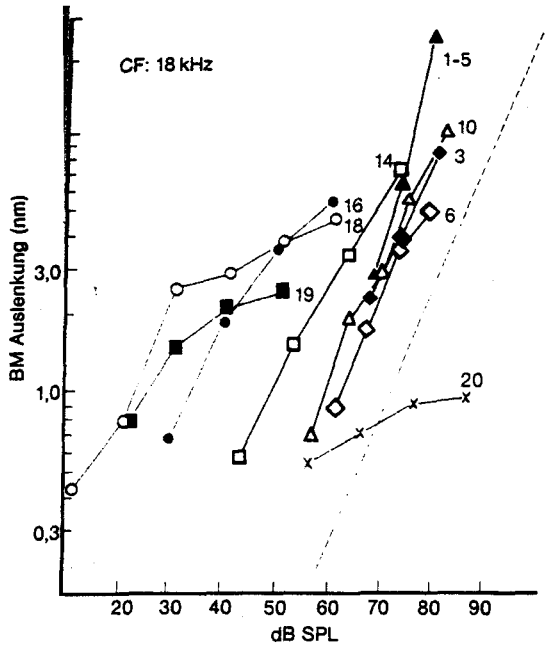

Abb. 1.**88** Nichtlinearität bei Bestfrequenz: Die Auslenkung der Basilarmembran als Funktion der Schallintensität zeigt nahe oder oberhalb der Bestfrequenz (18kHz) eine Nichtlinearität (rotbraun), dagegen eine lineare Antwort bei niedrigeren Frequenzen (schwarz). Die Frequenz, mit der stimuliert wurde, ist an den Kurven angegeben. Die gestrichelte Linie zeigt eine Kurve mit einer Steigung von 1, entsprechend einer linearen Antwort (nach Sellick u. Mitarb. [591]).

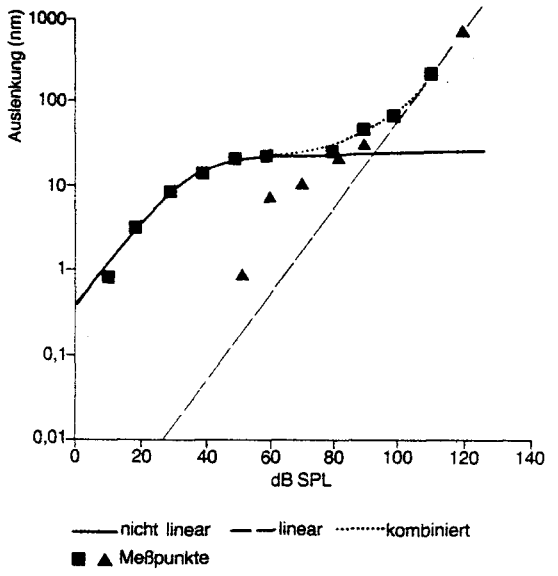

Abb. 1.**89** Das Ausmaß der Basilarmembranauslenkung als Funktion der Schallintensität:

- ■ Aktive Basilarmembranauslenkung einer Kochlea in physiologischem Zustand.
- ▲ Passive Basilarmembranauslenkung nach Schädigung durch akustisches Trauma.

Die durchgezogene Linie gibt das nichtlineare Verhalten der Basilarmembranantwort in der gesunden Kochlea wieder. Die gestrichelte Linie ist der Anteil der passiven, linearen Antwort: Die geschädigte Kochlea verhält sich fast linear, da der kochleäre Verstärker fehlt. Weiß ist die Fläche, die den Effekt des kochleären Verstärkers reflektiert (nach Johnstone u. Mitarb. [297]).

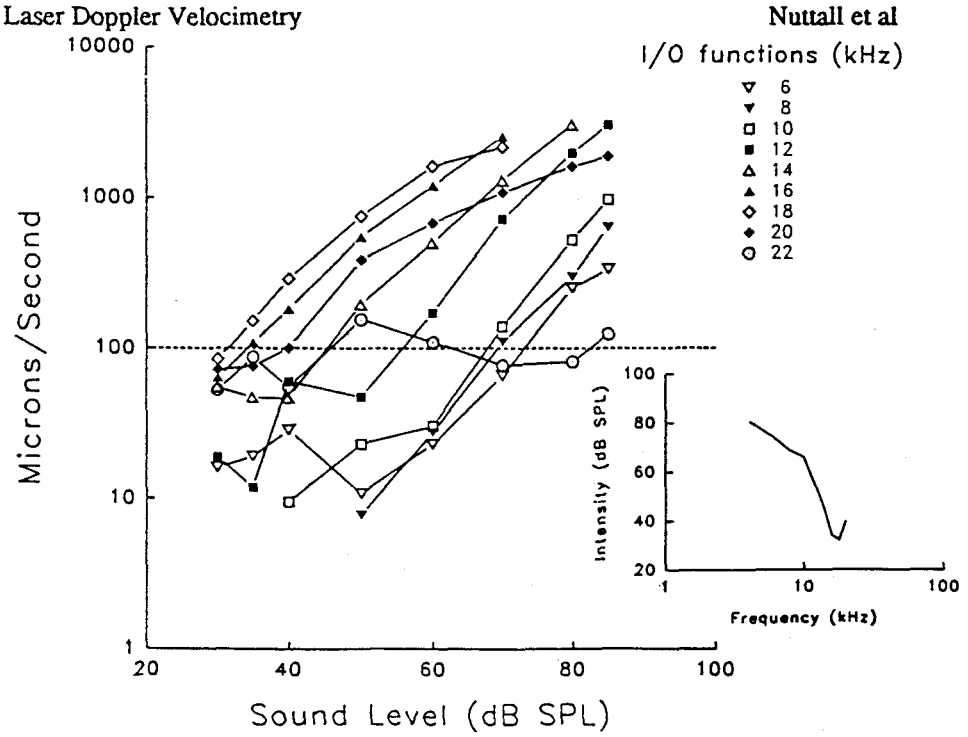

FIGURE 1. Intensity (input/output) functions obtained from a microbead located on the basilar membrane of the guinea pig. The characteristic frequency (CF) of the location was about 18.0 kHz. Intensity functions near the CF exhibit nonlinear (compressive) growth. The frequency tuning curve (insert) was derived from the input/output functions for a criterion of 100 microns/second.

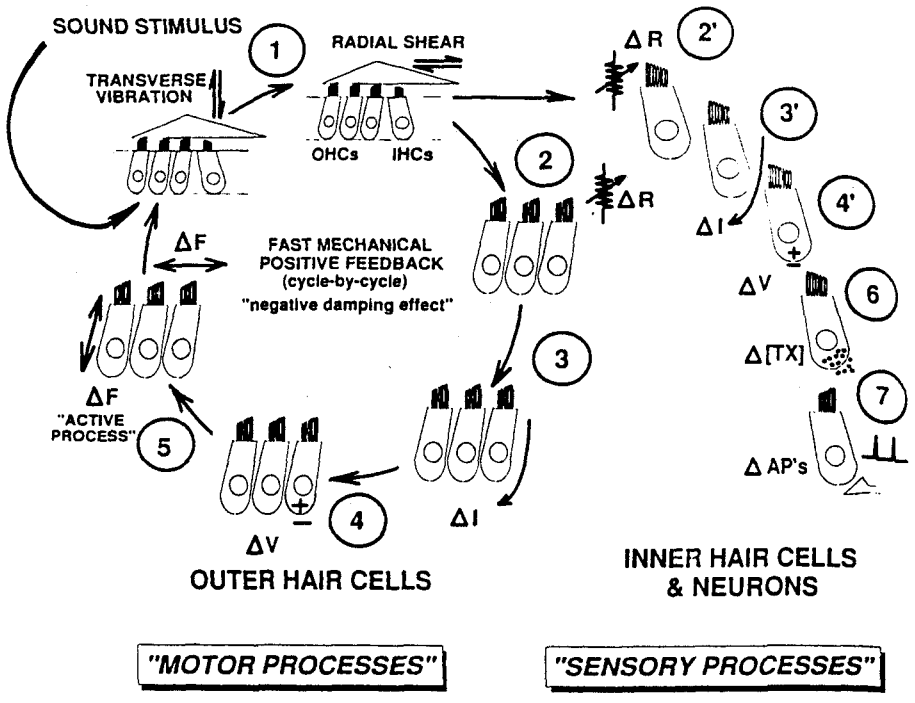

FIGURE 4.16 Transduction processes within the cochlea can conveniently be divided into "motor processes" that involve OHCs and enhance vibration of the cochlear partition, and "sensory processes" that involve IHCs and detect vibration by producing firing of primary afferent fibers. Many transduction processes are shared by the motor and sensory pathways: (1) Macromechanical and micromechanical vibration produce a relative shear stimulus to the hair bundles of the IHCs and OHCs. (2, 2') Deflection of hair bundles modulates electrical conductance (ΔR) at the apex of hair cells by opening and closing MET channels. (3, 3') Receptor currents (ΔI) flow due to this conductance change and the voltage across the apical membranes of the hair cells (endocochlear potential minus hair cell membrane potential). (4, 4') Receptor currents produce changes in cell membrane potentials [receptor potentials (ΔV)]. (5) In OHCs, the changes in membrane potential seem to control active forces (ΔF). (6) In IHCs, the membrane potentials control the release of neurotransmitter (Δ[TX]) and ultimately neural firing (ΔAPs) (7).

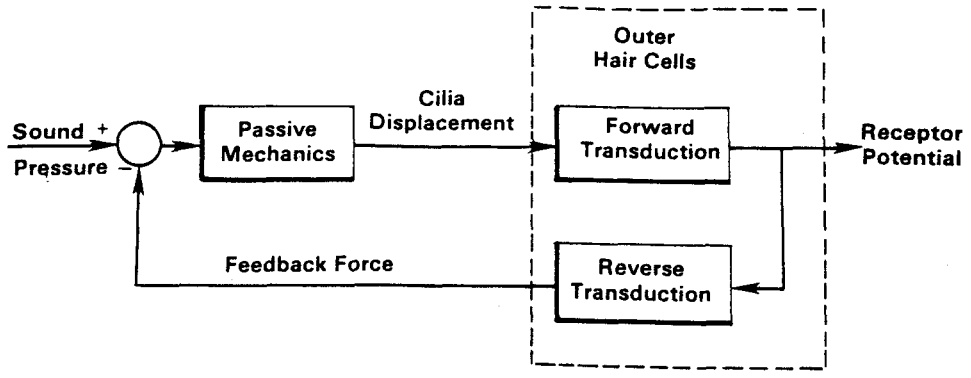

FIG. 2. Schematic diagram of the negative feedback model for outer hair cell function

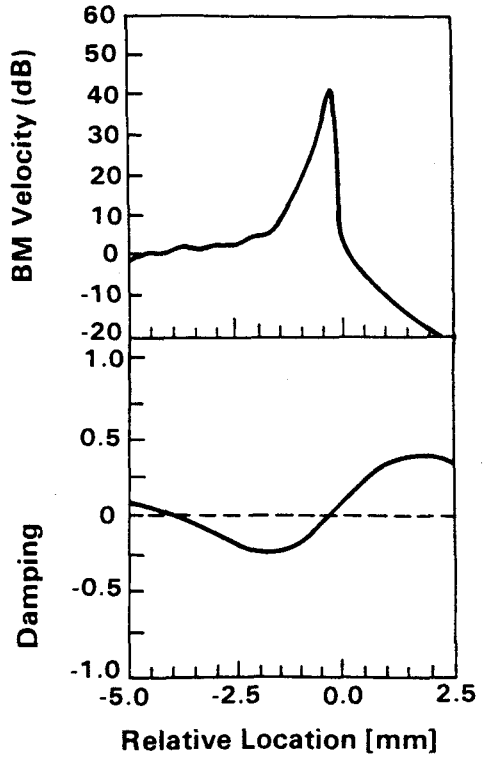

FIG. 3. Mechanical properties of the basilar membrane for a negative damping model. **A:** The envelope of the traveling wave as a function of basilar membrane location. **B:** The total damping of the cochlear partition as a function of position showing the region of negative damping which is basal to the traveling wave peak. (Adapted from de Boer, ref. 2)

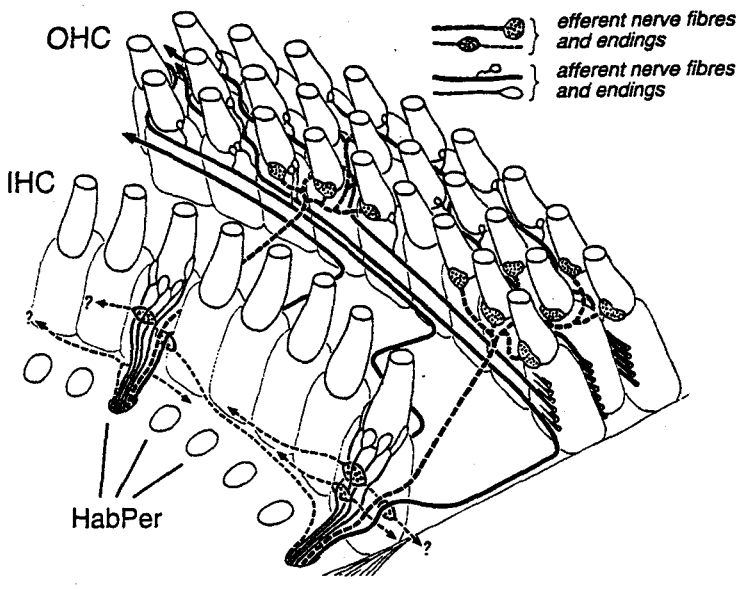

Figure 11.2. Cat organ of Corti showing the basic principles of its innervation with afferent and efferent neurons. The peripheral axon of each type I afferent neuron (thin solid line) enters through the habenula perforata (HabPer) and terminates in a single synapse on one inner hair cell (IHC). A type II afferent neuron sends its peripheral axon (thick solid line) on a spiral route that eventually innervates a group of outer hair cells (OHC). Efferent neurons (see Chapter 15) make multiple synapses with either a group of outer hair cells (thick dashed lines) or the peripheral axons of afferent neurons (thin dashed lines). Only representative examples of peripheral neurons arriving at the organ of Corti through two habenular openings are shown. (From Spoendlin, 1967, with permission.*)

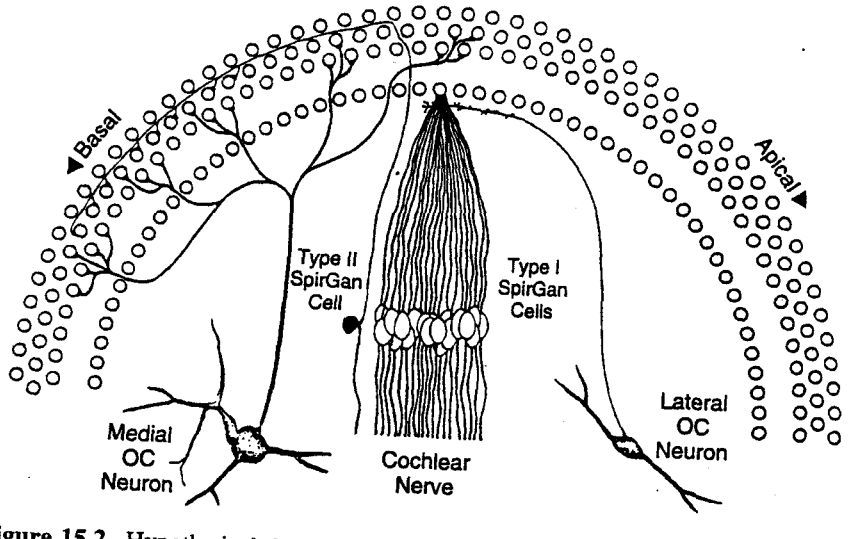

Figure 15.2. Hypothetical depiction of the afferent and efferent innervation related to a single mid-cochlear segment. Two types of afferent neurons (SpirGan) and two types of efferent neurons (OC) are tuned to the segment's frequency. Note the partial spatial overlap of the MOC efferent and type II afferent innervation patterns in the region immediately basal to the segment. The LOC neuron shown is of the "intrinsic" type. (From Warr, 1992, with permission.*)

Comparison of the OHC and the IHC subsystems in the caudal part of the auditory system from the cochlea up to the superior olivary complex

	OHC subsystem	IHC subsystem
Function	Biomechanical gain control	Usual sensory transduction
Role in cochlear biomechanics	Active	Passive
Enhanced sensitivity, tuning, dynamic range, & nonlinearity	Source	Beneficiary
Hair bundle re tectorial membrane	Firm attachment	Loose or no attachment
Hair cells	Many (12,000)	Few (3,500)
Afferent neurons	Few (2,100)	Many (27,900)
Efferent neurons	Large, myelinated	Small, unmyelinated
Afferent signal	Low spatial & temporal resolutions	High spatial & temporal resolutions
Efferent effect	Attenuation of cochlear mechanical response	Inhibition of radial nerve fibers
Physiological vulnerability	Highly vulnerable	Less vulnerable
Spont. rate (SR) of aff. neurons	Unknown	Bimodal distribution: 35%, SR 15 spikes/s 65%, SR 15 spikes/s

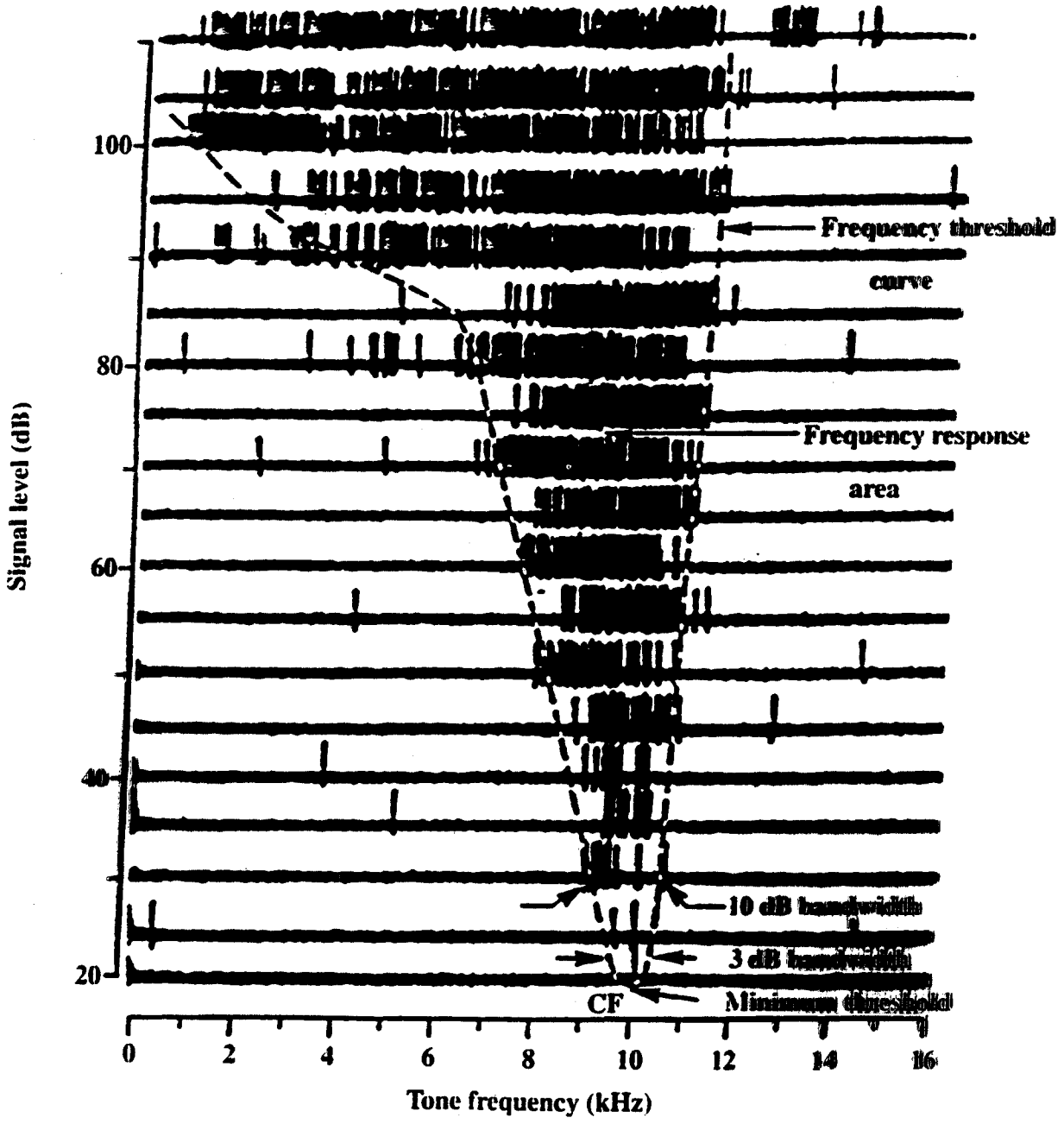
Signal level (dB)
100
80
60
40
20
Frequency threshold
curve
Frequency response
area
10 dB bandwidth
3 dB bandwidth
CF
Minimum threshold
0
2
4
6
8
10
12
14
16
Tone frequency (kHz)

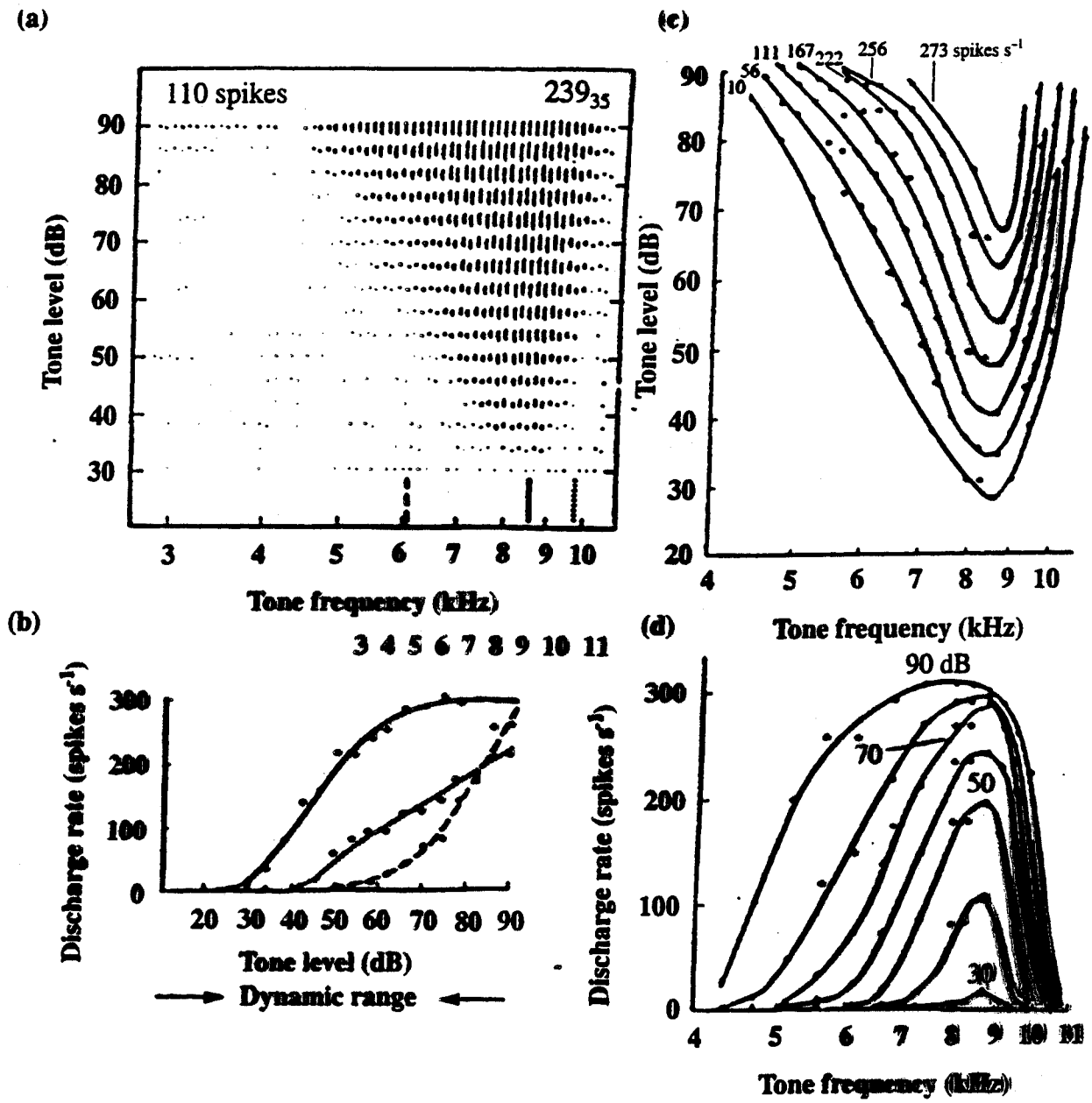
(a)
110 spikes
239_{35}
Tone level (dB)
Tone frequency (kHz)
(b)
Discharge rate (spikes s^{-1})
Tone level (dB)
Dynamic range
(c)
111 167 222 256 273 spikes s^{-1}
Tone level (dB)
Tone frequency (kHz)
(d)
90 dB
70
50
30
Discharge rate (spikes s^{-1})
Tone frequency (kHz)

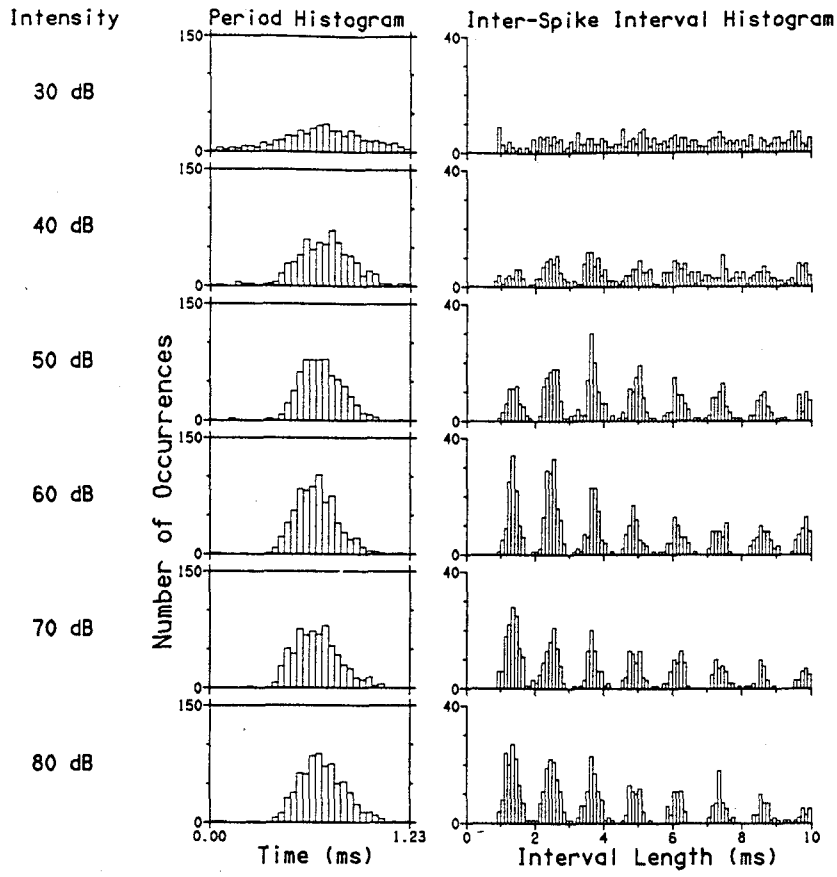

FIG. 3. Period and ISI histograms obtained in response to tones at 811 Hz, which was the fiber's CF, presented in 10-dB intensity steps.

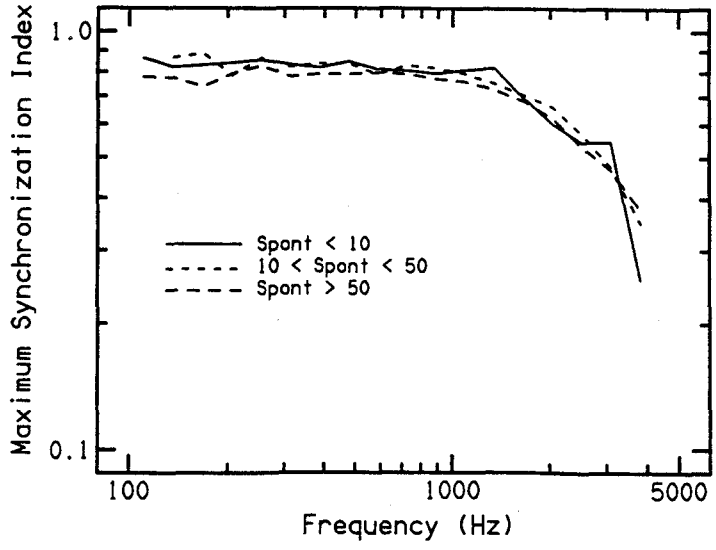

FIG. 4. Maximum synchronization as a function of frequency for auditory nerve fibers. Fibers have been partitioned into three groups based on spontaneous discharge rates.

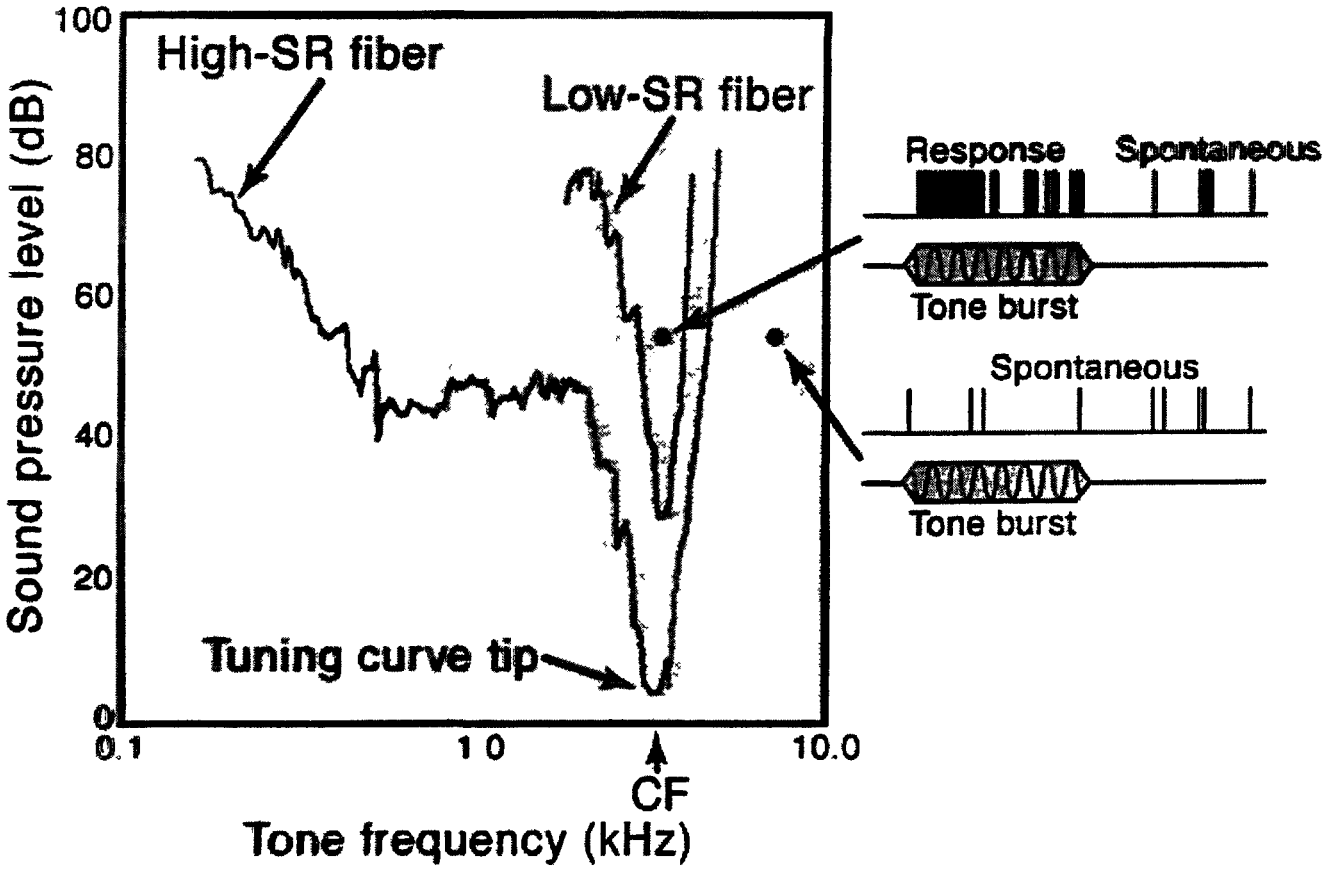

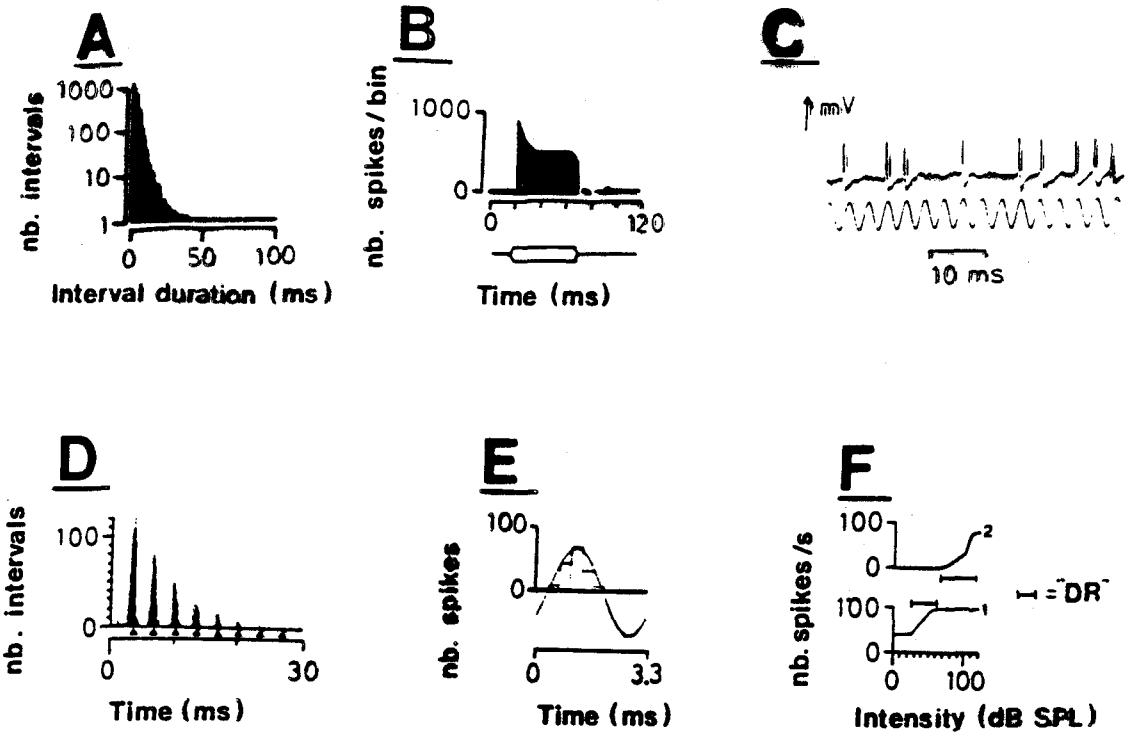
A
nb. intervals
1000
100
10
1
0
50
100
Interval duration (ms)
B
nb. spikes / bin
1000
0
0
120
Time (ms)
C
mV
10 ms
D
nb. intervals
100
0
0
30
Time (ms)
E
nb. spikes
100
0
0
3.3
Time (ms)
F
nb. spikes/s
100
0
100
0
0
100
Intensity (dB SPL)
DR

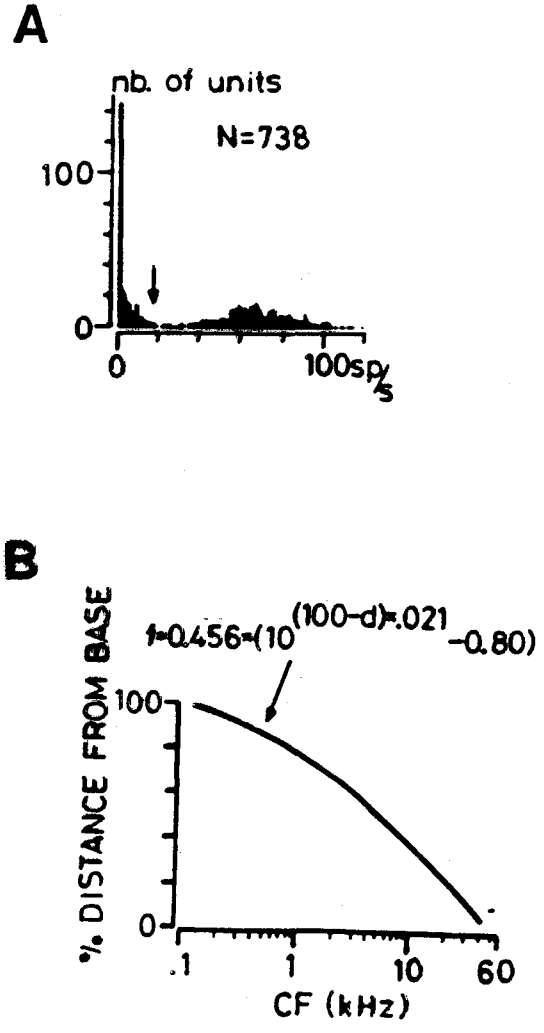
A
nb. of units
N=738
100
0
0
100sp/s
B
% DISTANCE FROM BASE
f=0.456-(10^((100-d)*.021)-0.80)
100
0
.1
1
10
60
CF (kHz)

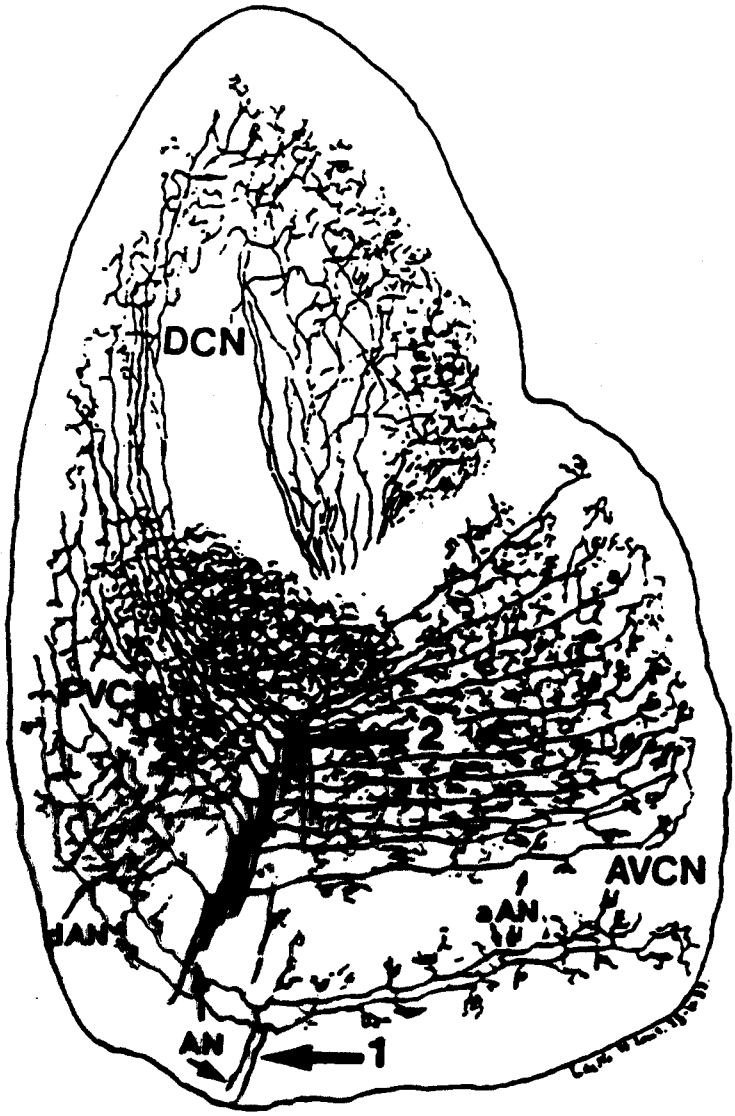
DCN
PVCN
AVCN
AN
AN
AN
1
2

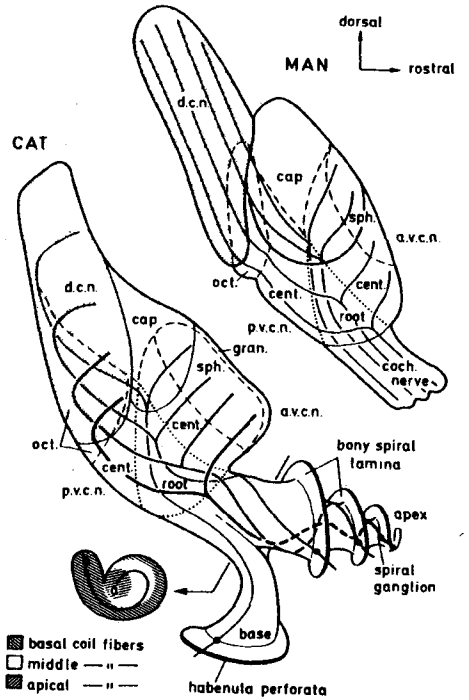

FIGURE 3.2. Lateral views of the cochlear nuclear complex of cat and man that illustrate the course of the cochlear nerve fibers from the spiral ganglion to their terminations in the complex. Axons enter the cochlear nuclear complex at its ventral aspect and bifurcate to form ascending and descending branches. The ascending branches pass through the length of the AVCN. The descending branches pass first through the PVCN and then enter the DCN. Abbreviations: DCN, dorsal cochlear nucleus; a.v.c.n., anteroventral cochlear nucleus; p.v.c.n., posteroventral cochlear nucleus; sph., spherical cell area, which occupies the anterior division of the AVCN (AVCN-A, cf. Fig. 3.1); cent., central part of the ventral cochlear nucleus, which comprises AVCN-P and PVCN-A (cf. Fig. 3.1); oct., octopus cell area, which occupies PVCN-P (cf. Fig. 3.1); cap, peripheral cap of small cells. The small diagram at the bottom left illustrates the arrangement of fibers from the base (b) to the apex (a) in the cochlea of the cat. These branch at different levels in the cochlear nucleus, giving rise to its tonotopic organization (Figs. 3.3 and 3.4). From A. Brodal, Neurological Anatomy, Oxford University Press, 1981. Used with permission. (Original figures appeared in Moore and Osen 1979, and Arnesen and Osen 1978.)

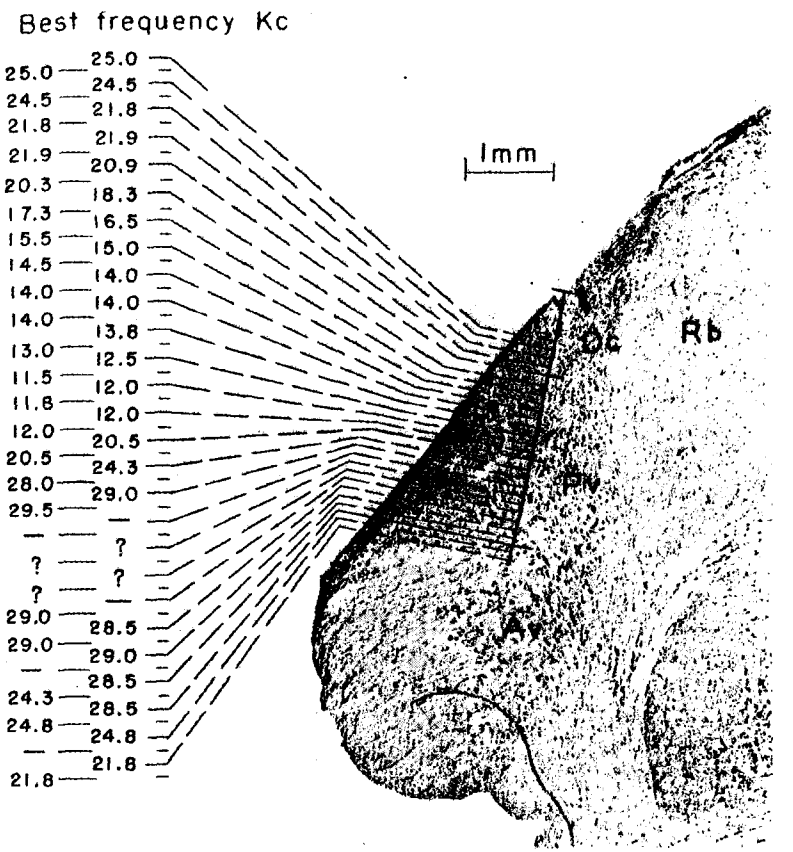

FIGURE 3.3. A section through the cochlear nucleus lying between the transver and horizontal planes. The dorsal aspect at the top of the section lies more po terior than the ventral aspect at the bottom. Medial is to the right. The appro imately vertical line drawn on the section represents the path of a recordir electrode through the nucleus. The numbers on the left indicate the best fr quencies of small clusters of units encountered at 50 μm steps. There is an order sequence from high to low best frequencies in the DCN (Dc) and a jump to high frequencies as the electrode enters the PVCN (Pv). Abbreviations: Av, antero entral cochlear nucleus; Rb, restiform body. [From Rose (1960); used with pe mission.]

1981; Kane, Puglisi, and Gordon 1981; Tolbert and Morest 1982a; r viewed by Cant and Morest 1984). Major neuronal classes are illustrate in Figure 3.5. There are two types of cells called bushy cells because the short primary dendrites give rise to a profusion of thin, lumpy appendag

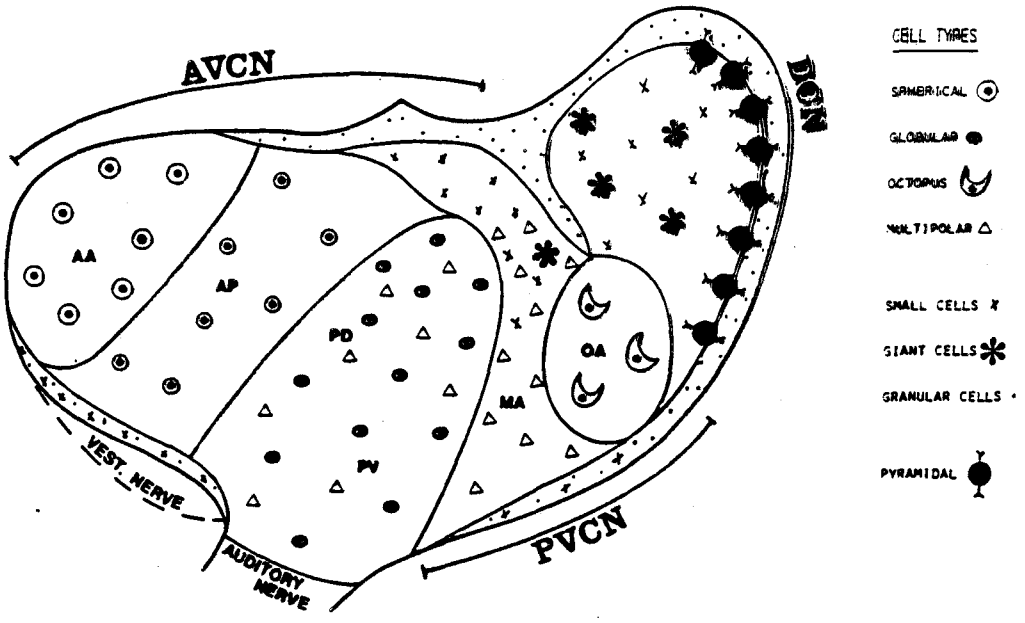
AVCN
DCN
PVCN
AA
AP
PD
PV
OA
MA
VEST. NERVE
AUDITORY NERVE
CELL TYPES
SPHERICAL
GLOBULAR
OCTOPUS
MULTIPOLAR
SMALL CELLS
GIANT CELLS
GRANULAR CELLS
PYRAMIDAL

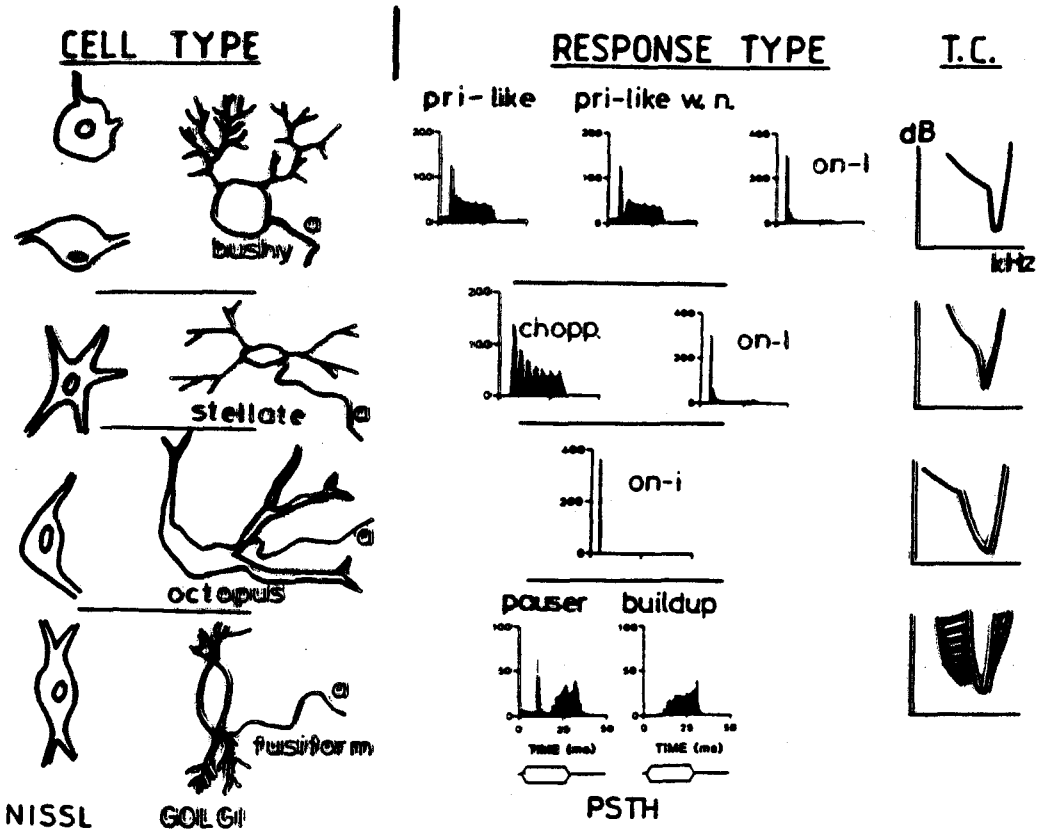
CELL TYPE
RESPONSE TYPE
T.C.
pri-like
pri-like w. n.
on-i
dB
kHz
bushy
chopp
on-i
stellate
on-i
octopus
pauser
buildup
fusiform
TIME (ms)
TIME (ms)
NISSL
GOLGI
PSTH

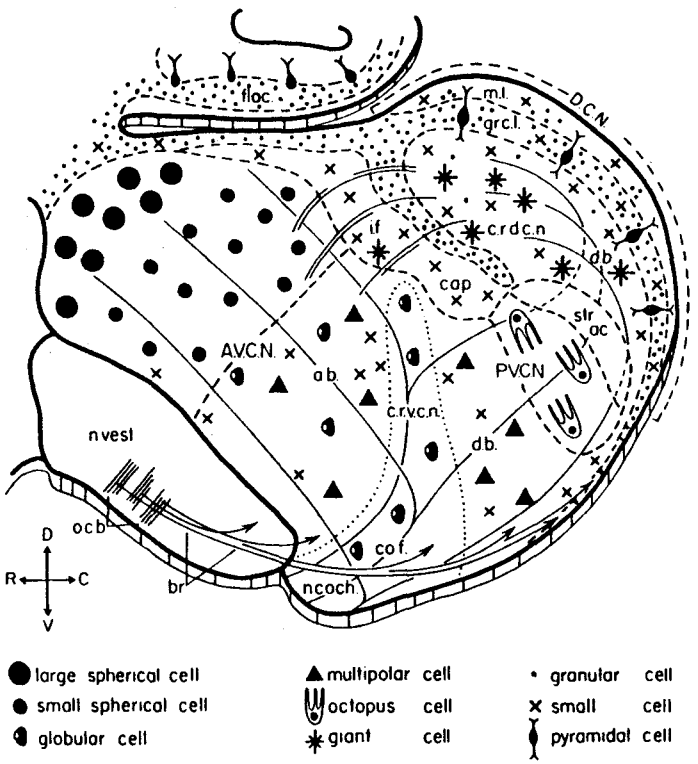

Fig. 6.2 A cytoarchitectural map of the cochlear nucleus is shown in sagittal section. The predominant cell types in each region are represented. AVCN, anteroventral nucleus; cap, peripheral cap of small cells; crdcn, central region of DCN; crcvn, central region of ventral nucleus; DCN, dorsal nucleus; floc, flocculus (cerebellum); gcl, granular cell layer; if, intrinsic fibres; ml, molecular layer; PVCN, posteroventral nucleus; strac, dorsal and intermediate acoustic striae. From Osen and Roth (1969, Fig. 1).

aspartate are often suggested (e.g. Godfrey *et al.*, 1984; Martin, 1985). The evidence is derived from high levels of the amino acids and their associated enzymes in the auditory nerve root, and the effects of the acids and their agonists and antagonists on cells of the cochlear nucleus. The evidence has been reviewed by Wenthold and Martin (1984).

GABA (γ-amino butyric acid) and glycine may be inhibitory transmitters, particularly in the DCN, and associated with interneurones (Godfrey *et al.*, 1978; Peyret *et al.*, 1987). Glycine has also been suggested as the transmitter of fibres which run directly between the cochlear nuclei of the two sides

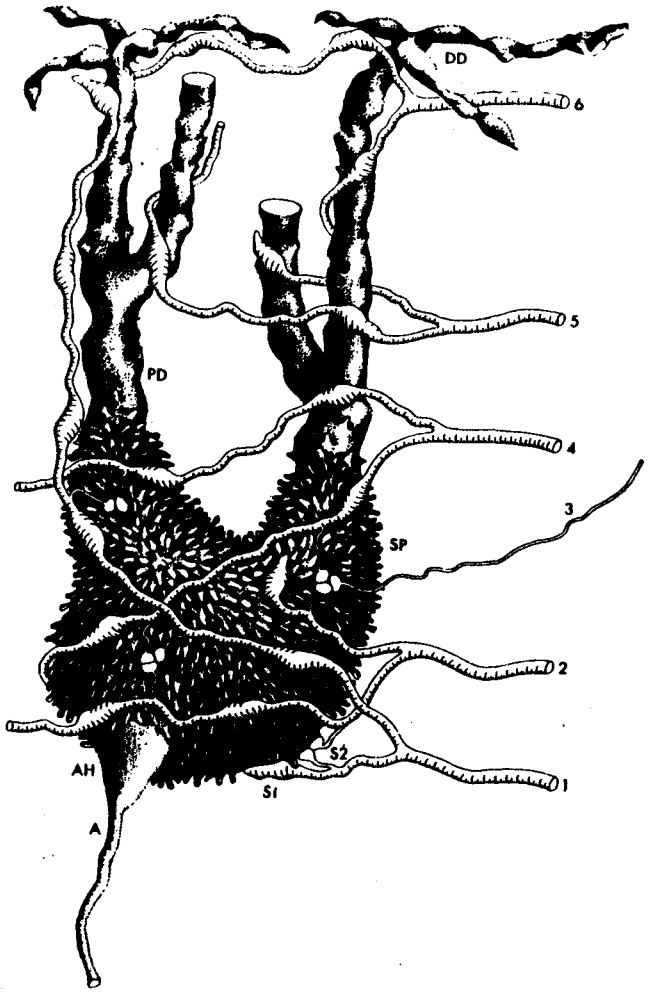

Fig. 6.3 An octopus cell. The thick auditory nerve fibres (1,2,4,5,6) give rise to large endings (S1) on the cell. They may also branch to give thin fibres, which, together with thin afferent axons (3) give rise to small secondary endings (S2). The cell is covered with stubby appendages (SP). AH, axon hillock; A, axon. From Morest *et al.* (1973, Fig. 2).

(Wenthold, 1987). Acetylcholine and noradrenaline in the cochlear nuclei are thought to be mainly transmitters of the centrifugal, or "descending", innervation arising from the central nervous system. These will be discussed further in Chapter 8.

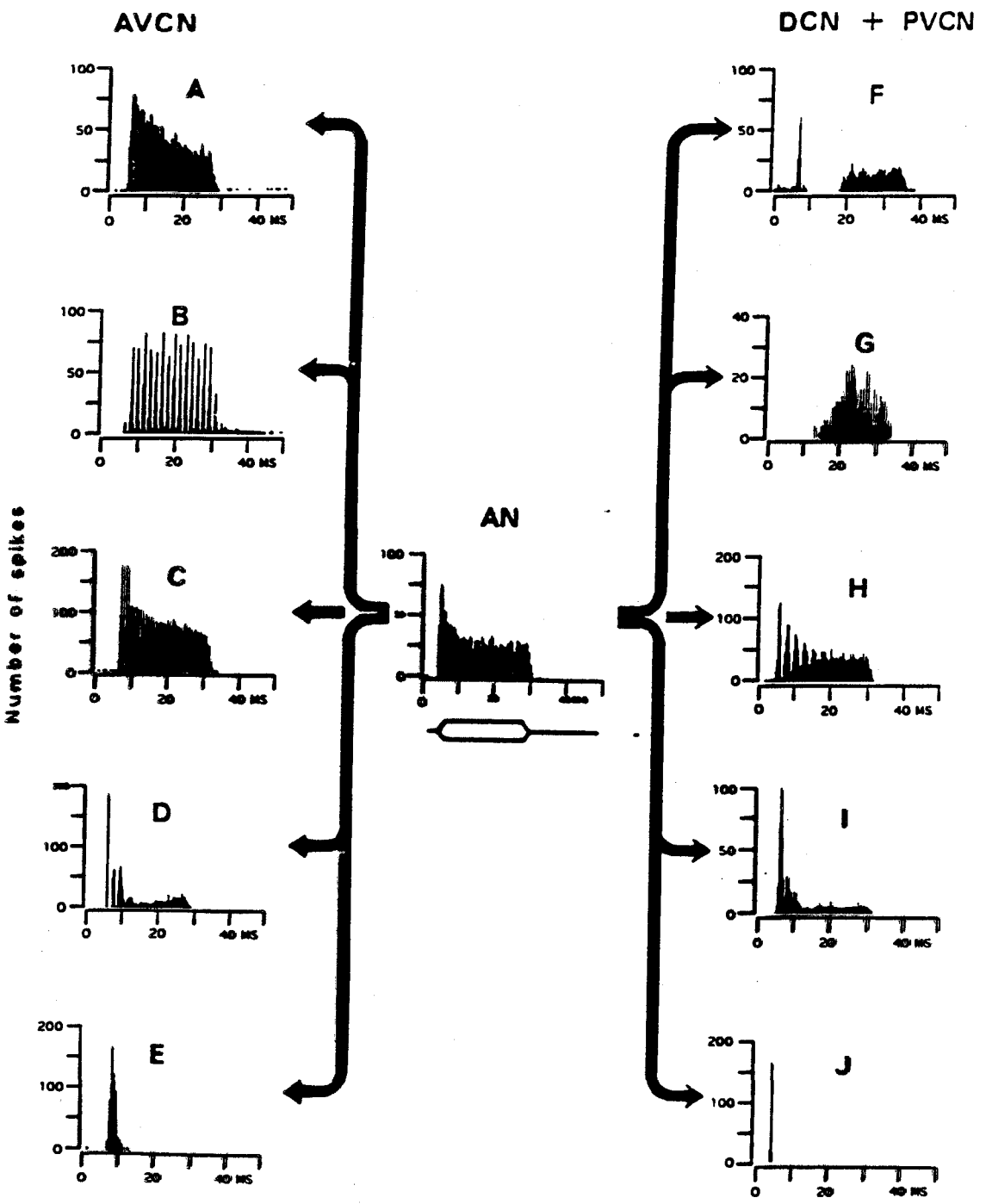
AVCN
DCN + PVCN
A
B
C
D
E
F
G
H
I
J
AN
Number of spikes
0
20
40 MS

FIG 27.12

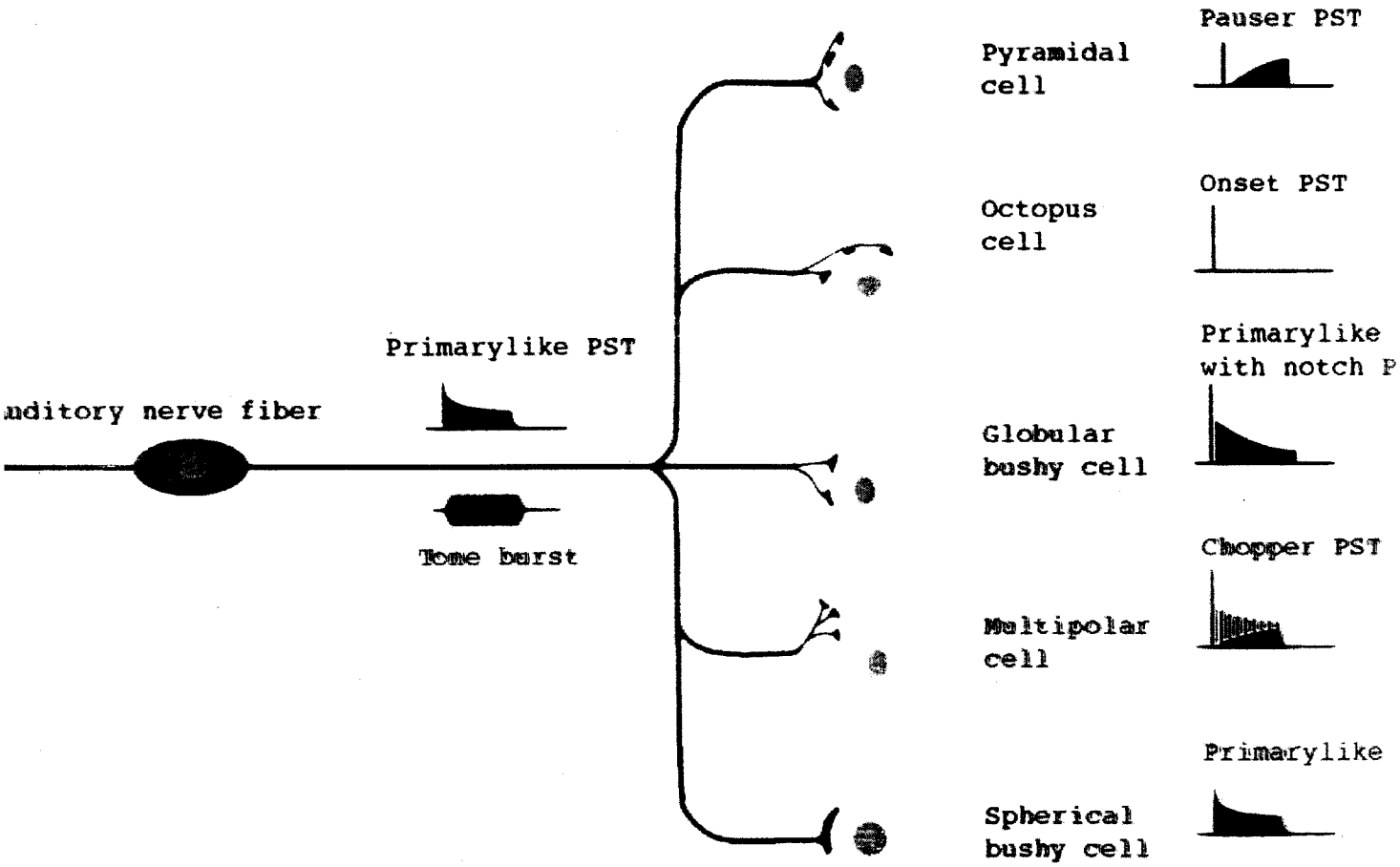

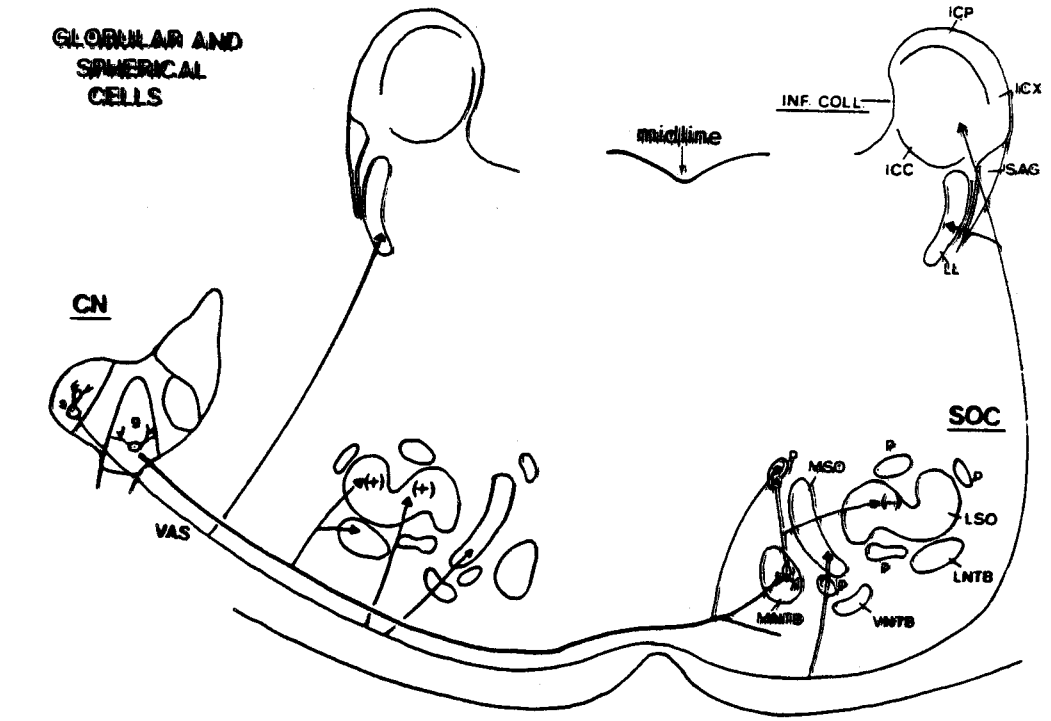
GLOBULAR AND
SPHERICAL
CELLS
ICP
INF. COLL.
ICX
midline
ICC
SAG
LL
CN
SOC
MSO
LSO
LNTB
MNTB
VNTB
VAS

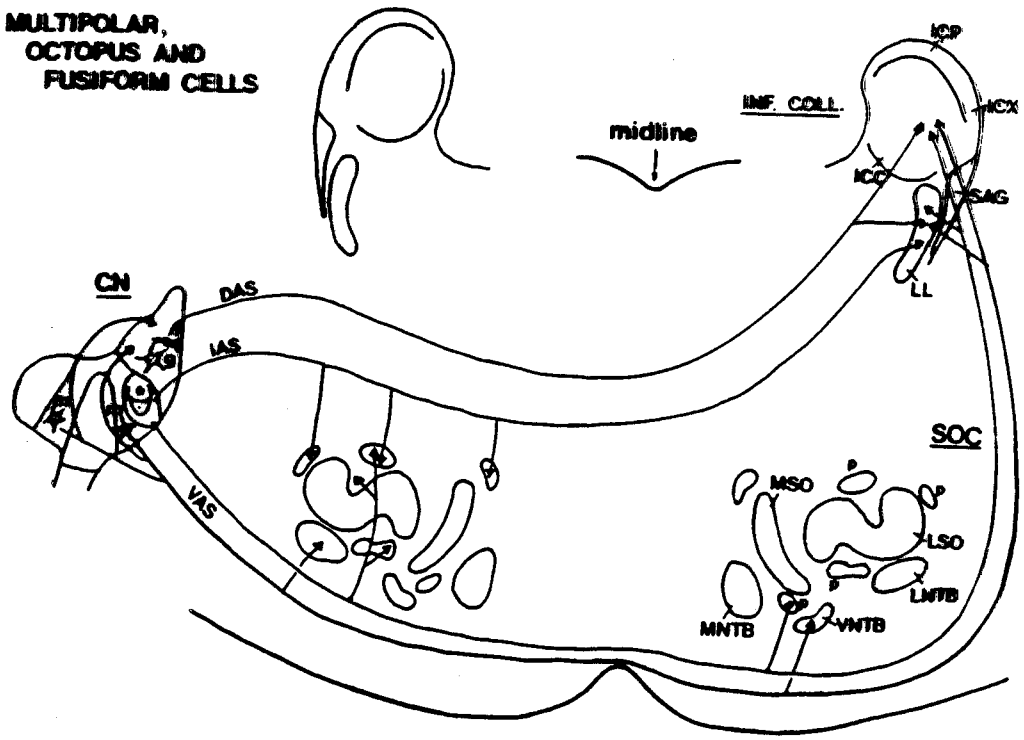
MULTIPOLAR,
OCTOPUS AND
FUSIFORM CELLS
ICP
INF. COLL.
ICX
midline
ICC
SAG
LL
CN
DAS
IAS
VAS
SOC
MSO
LSO
LNTB
MNTB
VNTB

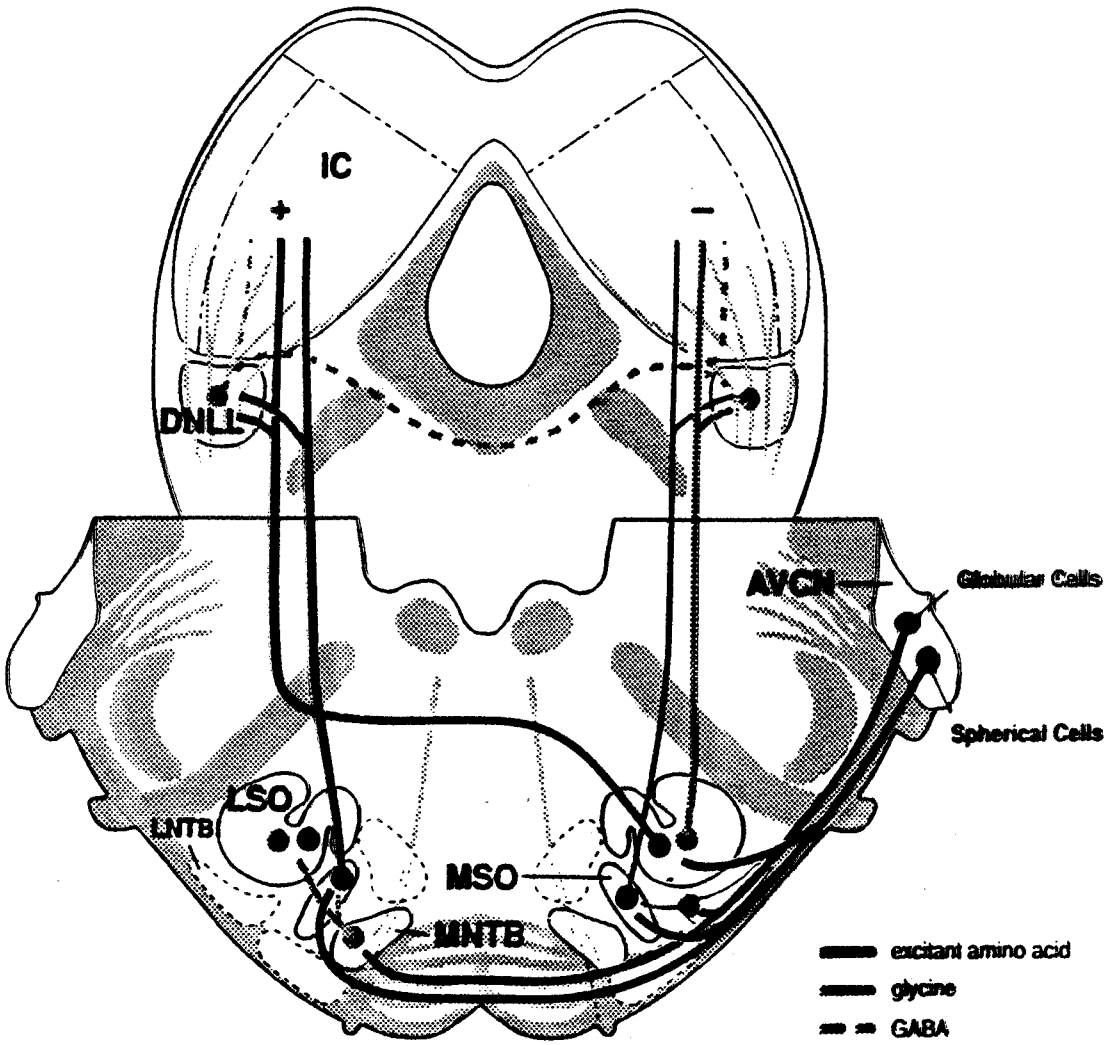
IC
+
−
DNLL
AVCN
Globular Cells
Spherical Cells
LSO
LNTB
MSO
MNTB
excitant amino acid
glycine
GABA

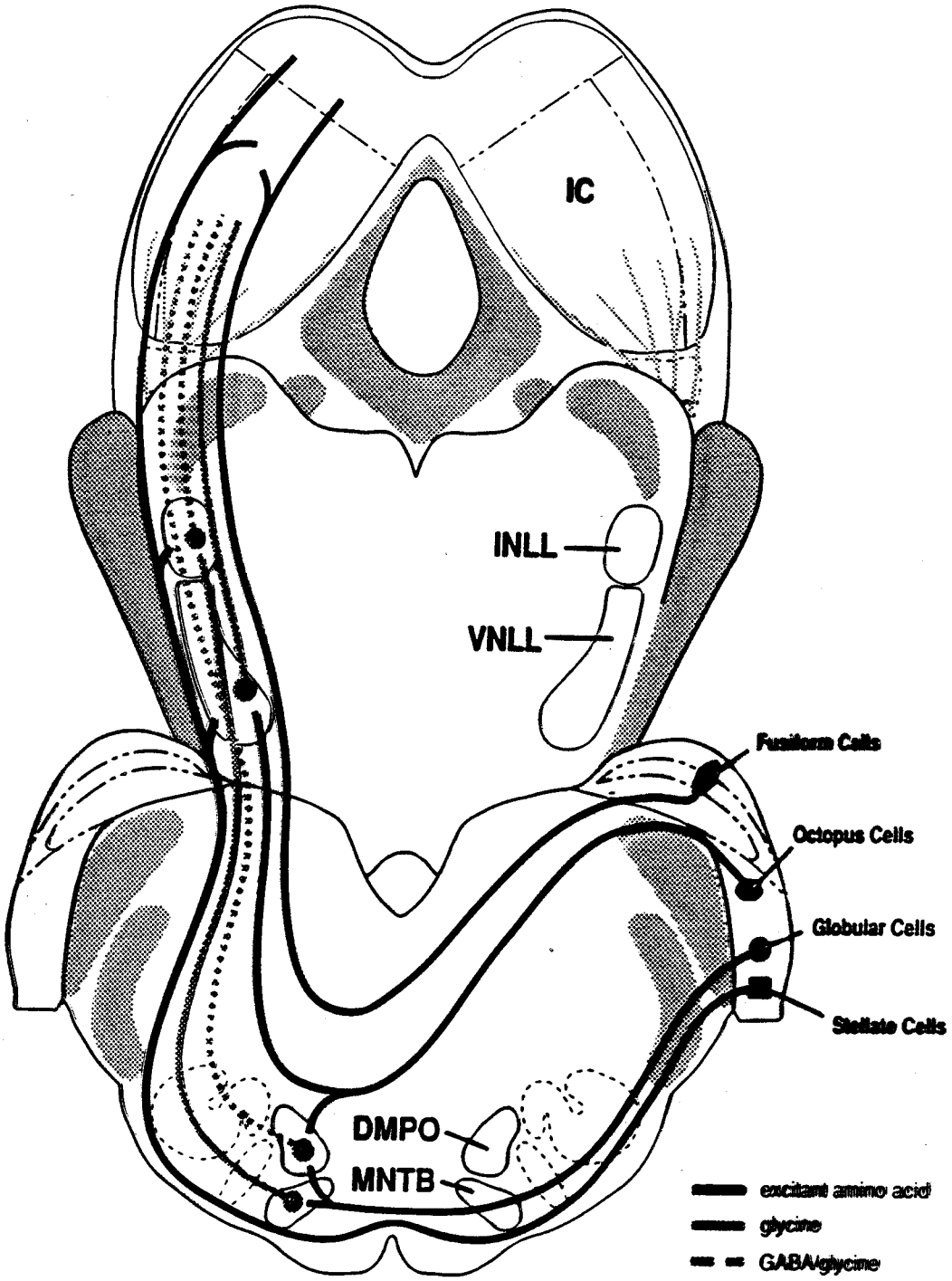
IC
INLL
VNLL
Fusiform Cells
Octopus Cells
Globular Cells
Stellate Cells
DMPO
MNTB
excitant amino acid
glycine
GABA/glycine

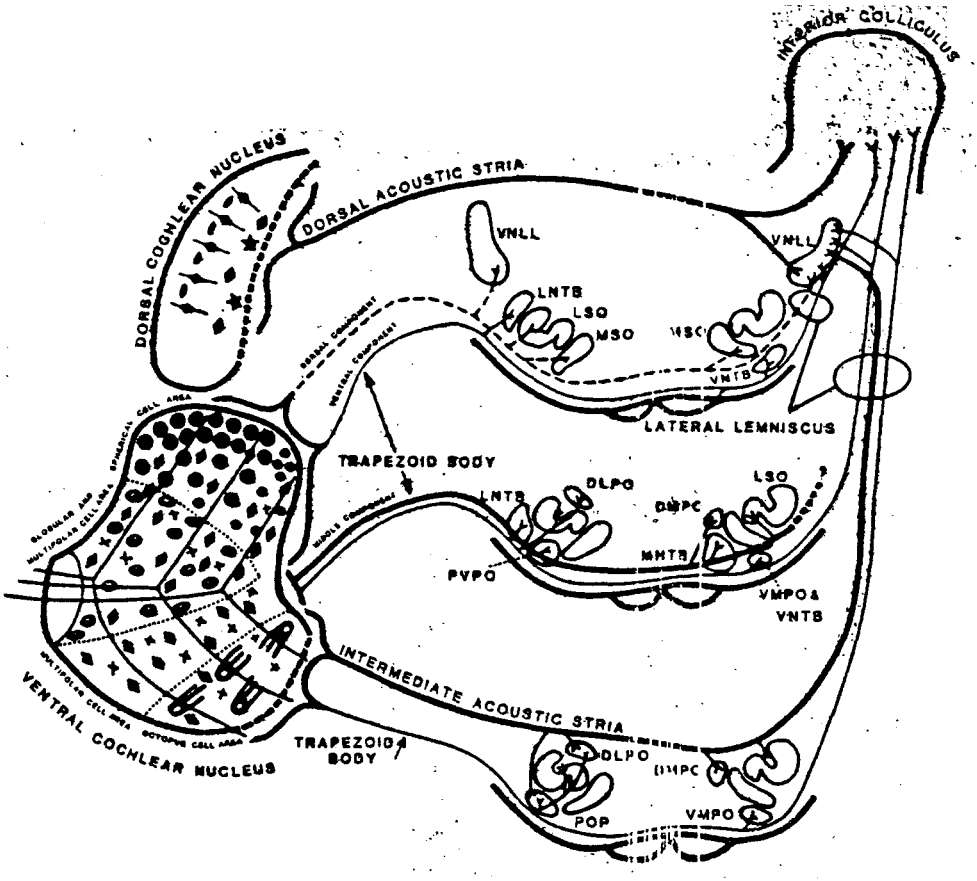

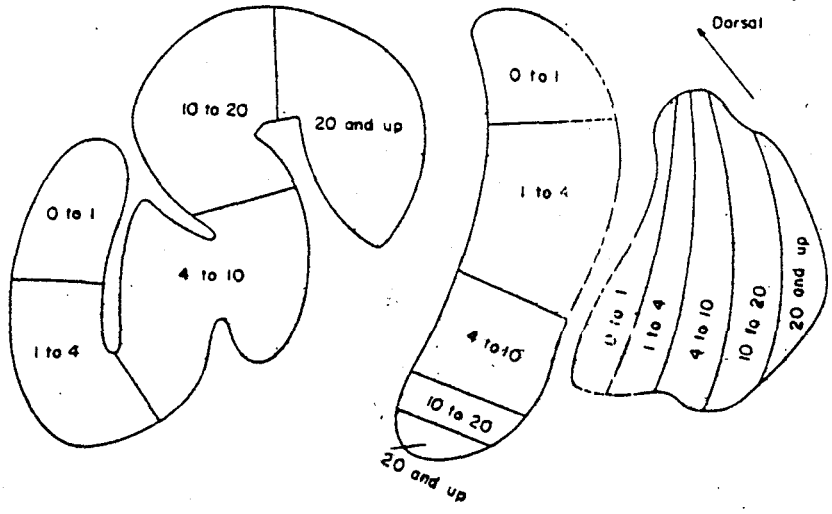

FIGURE 4.6. Tonotopic organization of the cat SOC from Figure 21, Guinan, Norris, and Guinan (1972), reprinted with permission of Gordon and Breach Science Publishers Ltd.

Simple differences in the connections to different MSO and LSO neuronal types can explain differences in their function. Some MSO and LSO principal cells are most sensitive to particular interaural phase differences, others to interaural intensity differences (Masterton et al. 1975; Heffner and Heffner 1986; Yin and Chan 1988). Single MSO neurons receiving high security synaptic input from spherical cells in both AVCNs are particularly suited to perform interaural phase analysis. MSO multiplanar

FIG 27.16

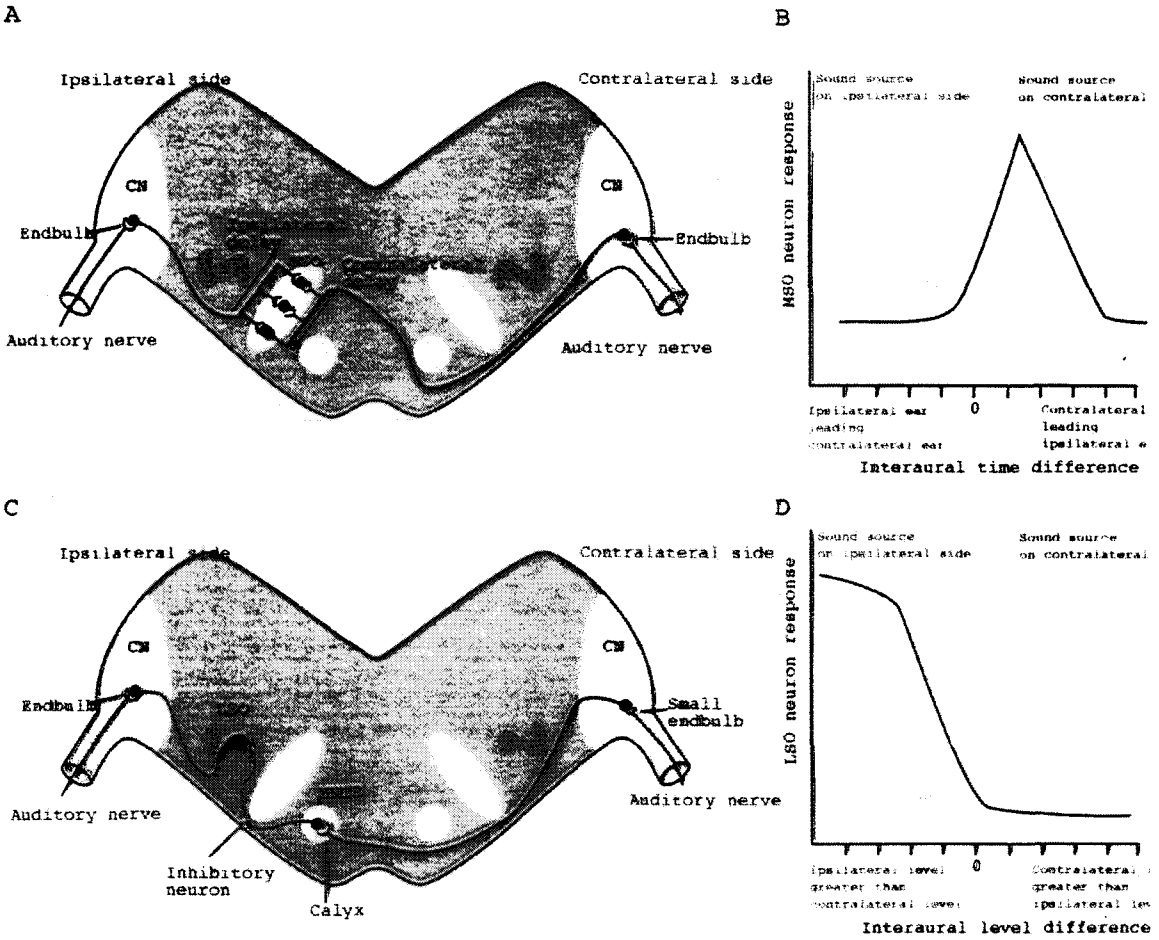

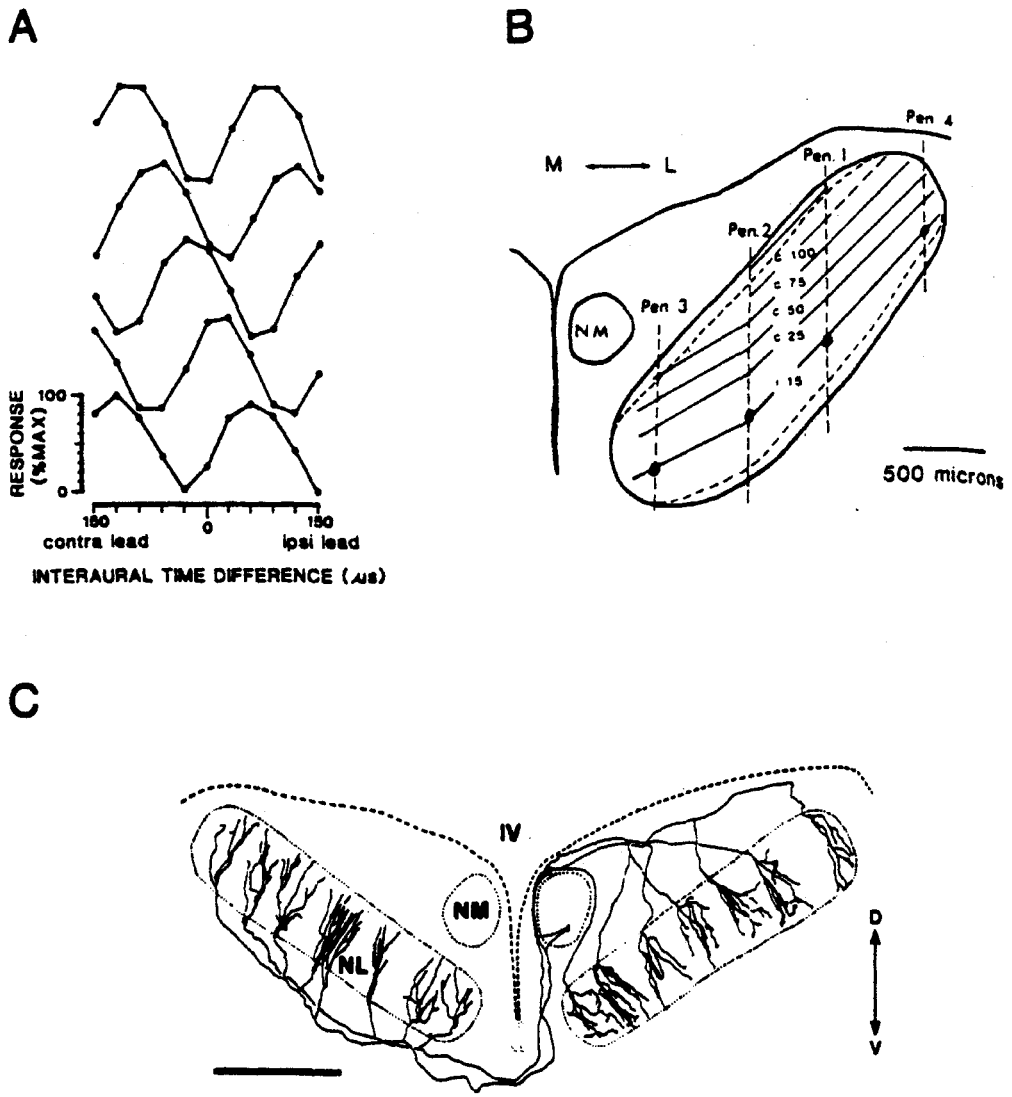

FIGURE 4.9. Topographic organization of interaural delay sensitivity, and its anatomical substrates, in the nucleus laminaris of the barn owl. (A) Interaural delay sensitivity curves for the neurophonic response as a function of recording depth in a penetration from dorsal (top trace) to ventral (bottom trace) through the nucleus laminaris, of the type illustrated in (B). Note the systematic shift in the interaural delay eliciting maximum response as a function of depth. (B) Map of interaural delay sensitivity in the nucleus laminaris derived from four penetrations (Pen 1–Pen 4) yielding data of the type shown in (A). Isodelay contours were derived by joining the points in each penetration at which the interaural delay specified on the contour (as contra or ipsi lead in μsec) produced maximum discharge (i.e., resulted in coincidence of monaural responses). L, lateral; M, medial; NM, nucleus magnocellularis. (Modified from Sullivan and Konishi 1986.) (C) Projections from the nucleus magnocellularis (NM) to the nucleus laminaris (NL) in the barn owl. The axons were labeled after a small injection of horseradish peroxidase into the 5.5-kHz region of the nucleus laminaris. The

FIG 27.6

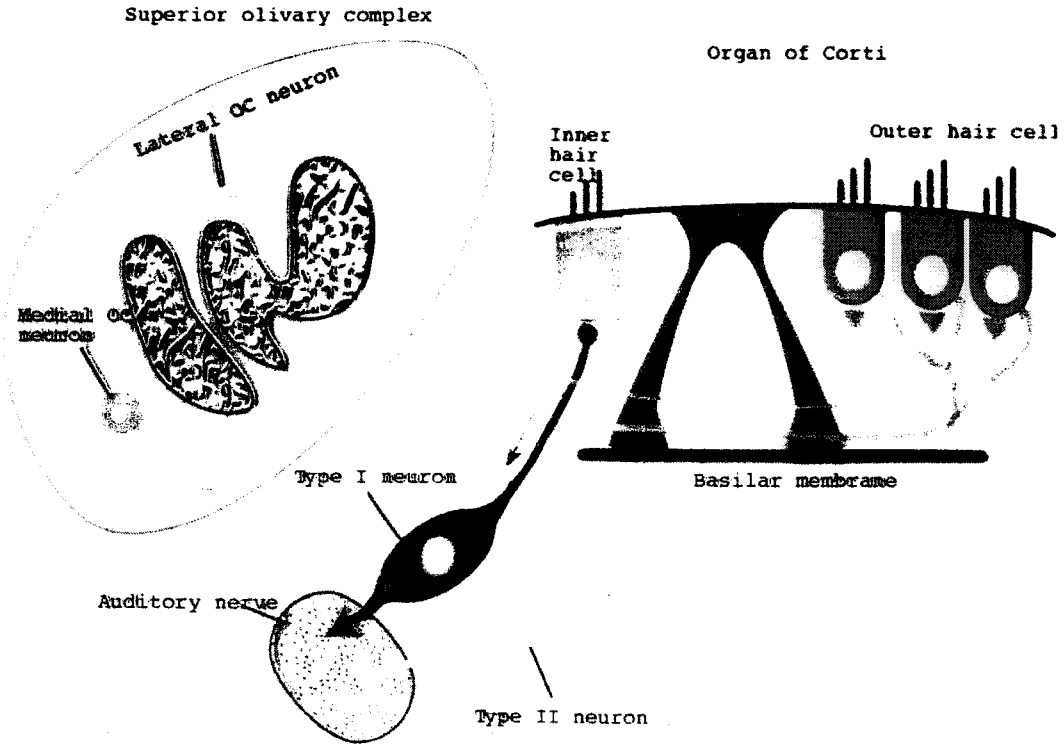

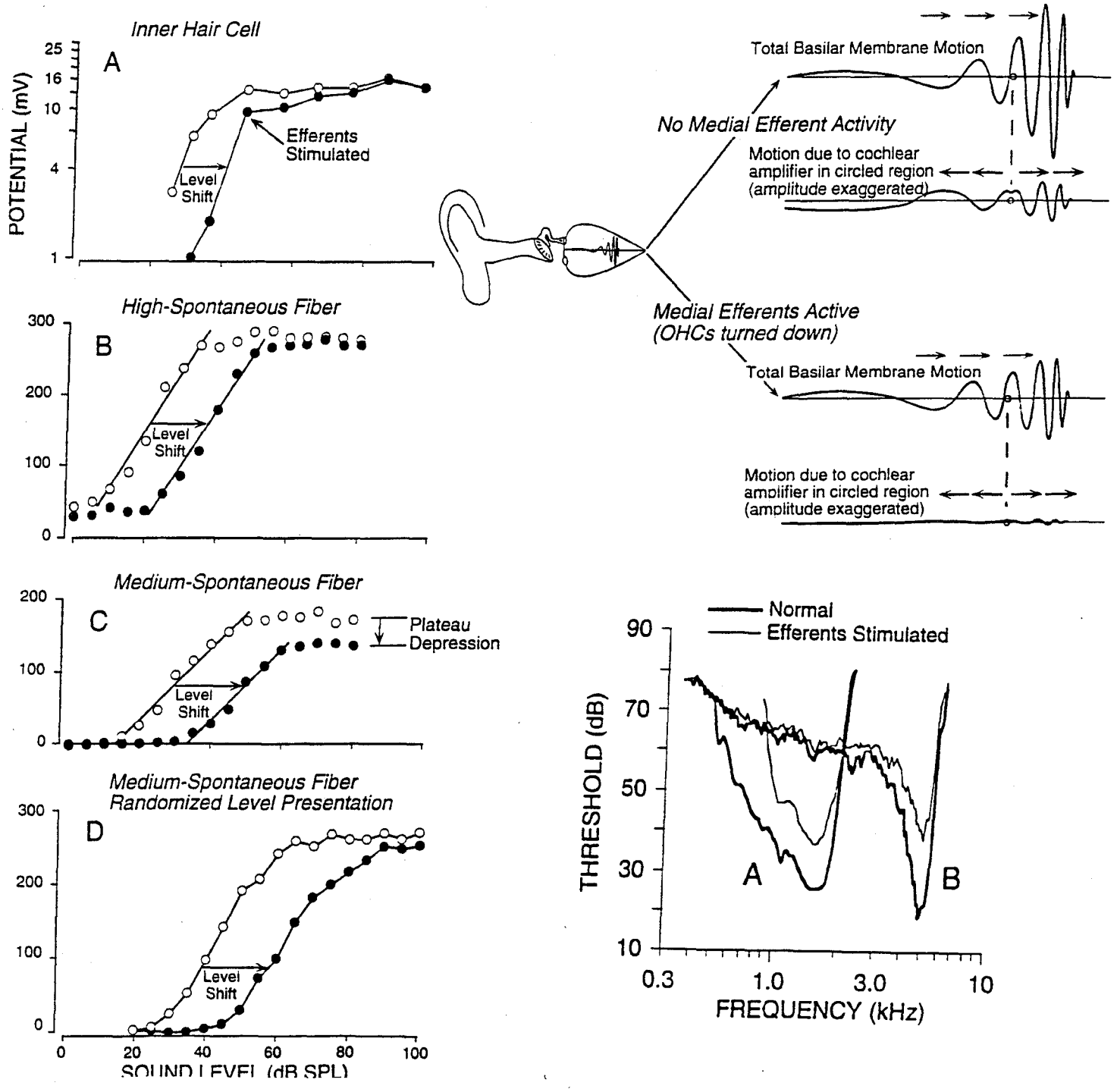
Inner Hair Cell
A
POTENTIAL (mV)
25
16
10
4
1
Efferents Stimulated
Level Shift
High-Spontaneous Fiber
B
300
200
100
0
Level Shift
Medium-Spontaneous Fiber
C
200
100
0
Plateau Depression
Level Shift
Medium-Spontaneous Fiber
Randomized Level Presentation
D
300
200
100
0
Level Shift
0
20
40
60
80
100
SOUND LEVEL (dB SPL)
No Medial Efferent Activity
Total Basilar Membrane Motion
Motion due to cochlear amplifier in circled region (amplitude exaggerated)
Medial Efferents Active (OHCs turned down)
Total Basilar Membrane Motion
Motion due to cochlear amplifier in circled region (amplitude exaggerated)
Normal
Efferents Stimulated
THRESHOLD (dB)
90
70
50
30
10
A
B
0.3
1.0
3.0
10
FREQUENCY (kHz)

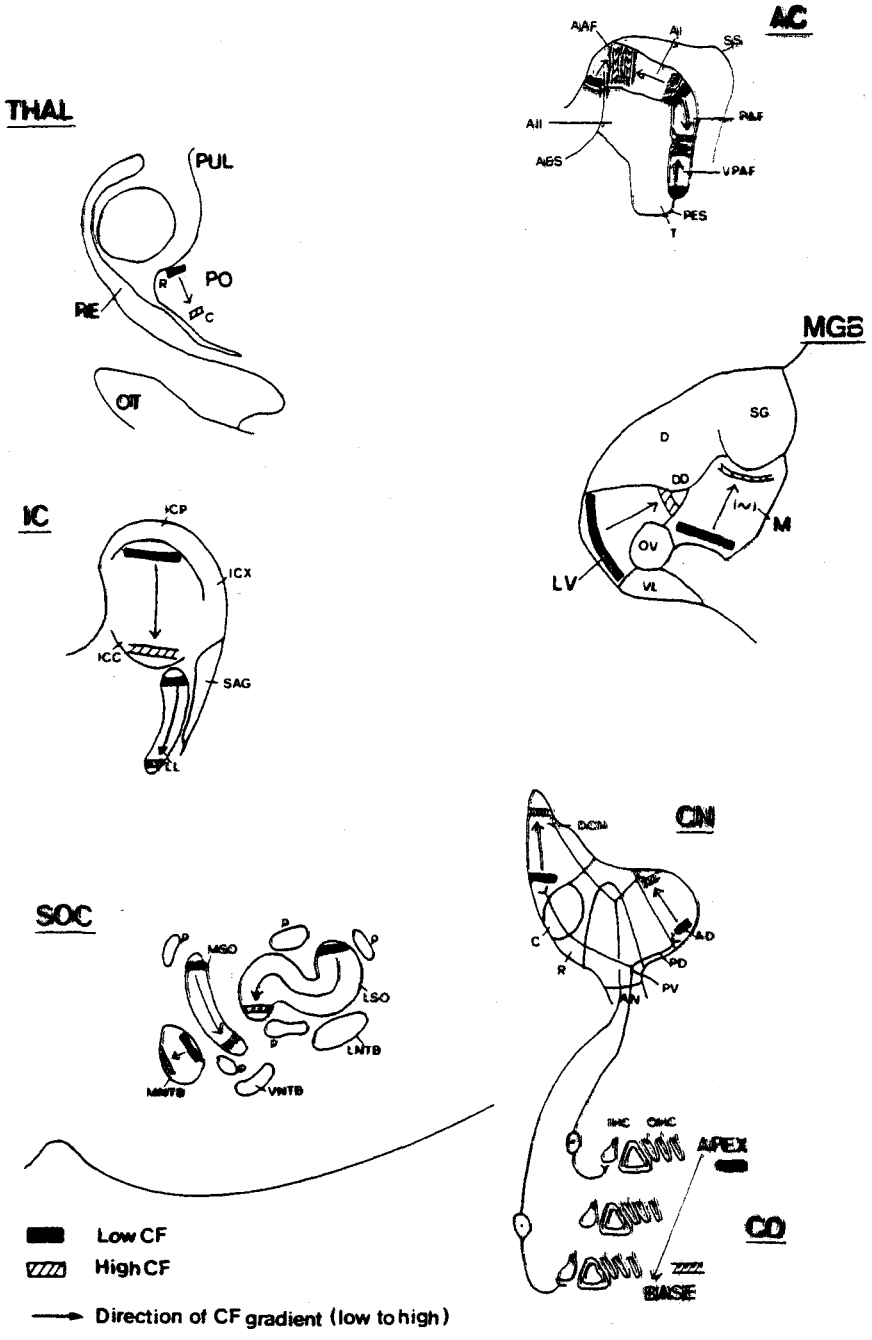

Figure 1.8. Schematic representation of the various auditory nuclei (in the cat) from the cochlear nucleus to the auditory cortex, with illustration of their respective tonotopic organization (preferential spatial arrangement of the neurons with respect to their CF). The arrows indicate the direction of the increasing CF gradients (isofrequency contours would therefore be perpendicular to the arrows). The black

FIG. 1. Subdivisions of the inferior colliculus in the cat stained with the Golgi-Cox method. This transverse section is in the middle of the colliculus, just caudal to the commissure. This plane of section (anatomical transverse) is perpendicular to the floor of the fourth ventricle. Age 2 months. (For abbreviations, see Table 1.) (From ref. 42, with permission.)

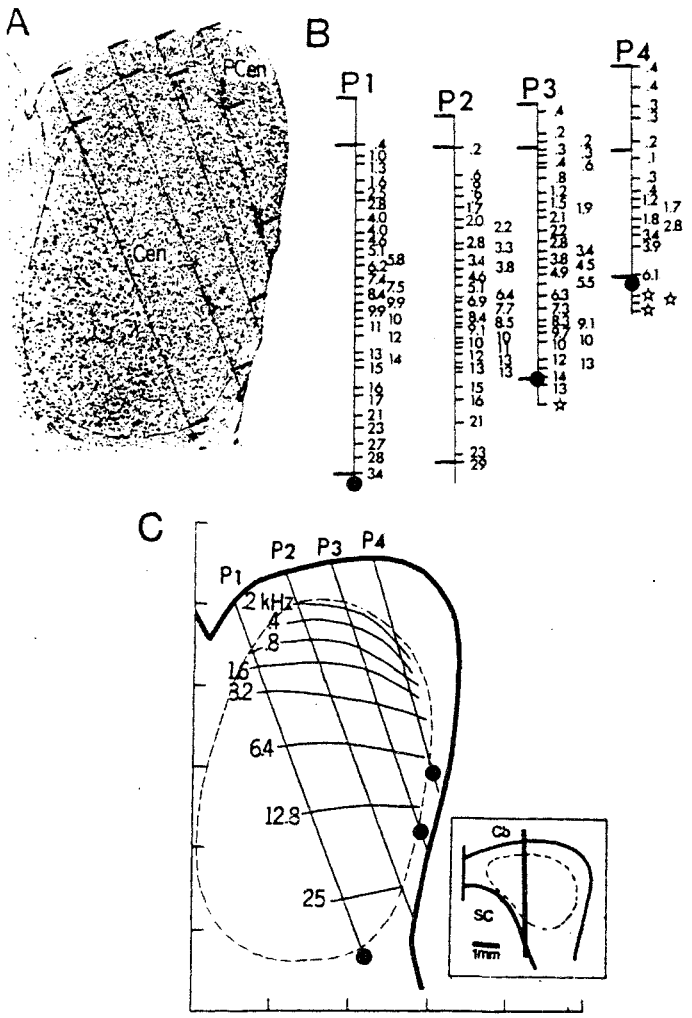

FIGURE 111. A, Sagittal section of the inferior colliculus at the location shown in the inset of C (right = caudal; left = rostral). Four microelectrode paths are shown. The cross bars at the paths mark the border between the central nucleus (Cen) and the pericentral areas (PCen). The approximate border line of the central nucleus is indicated by a dashed line. B, Reconstruction of the 4 electrode paths shown in A. Again, the heavy cross bars mark the borders of the central nucleus. The numbers give the characteristic frequencies in kHz of single units or groups of units found at those places marked by light cross bars. At those locations marked with an asterisk a response of the unit was obtained only with very high stimulus intensities. The filled circles show the locations at which the position of the electrode was marked by a lesion. C, Schematic presentation of iso-frequency contours thus obtained for characteristic frequencies. The iso-frequency contours are spaced at intervals of 1 octave and run parallel to the cellular laminae. Cb = cerebellum, SC = superior colliculus. (According to Merzenich and Reid [758].)

3

Spectro–Temporal Reverse Correlation

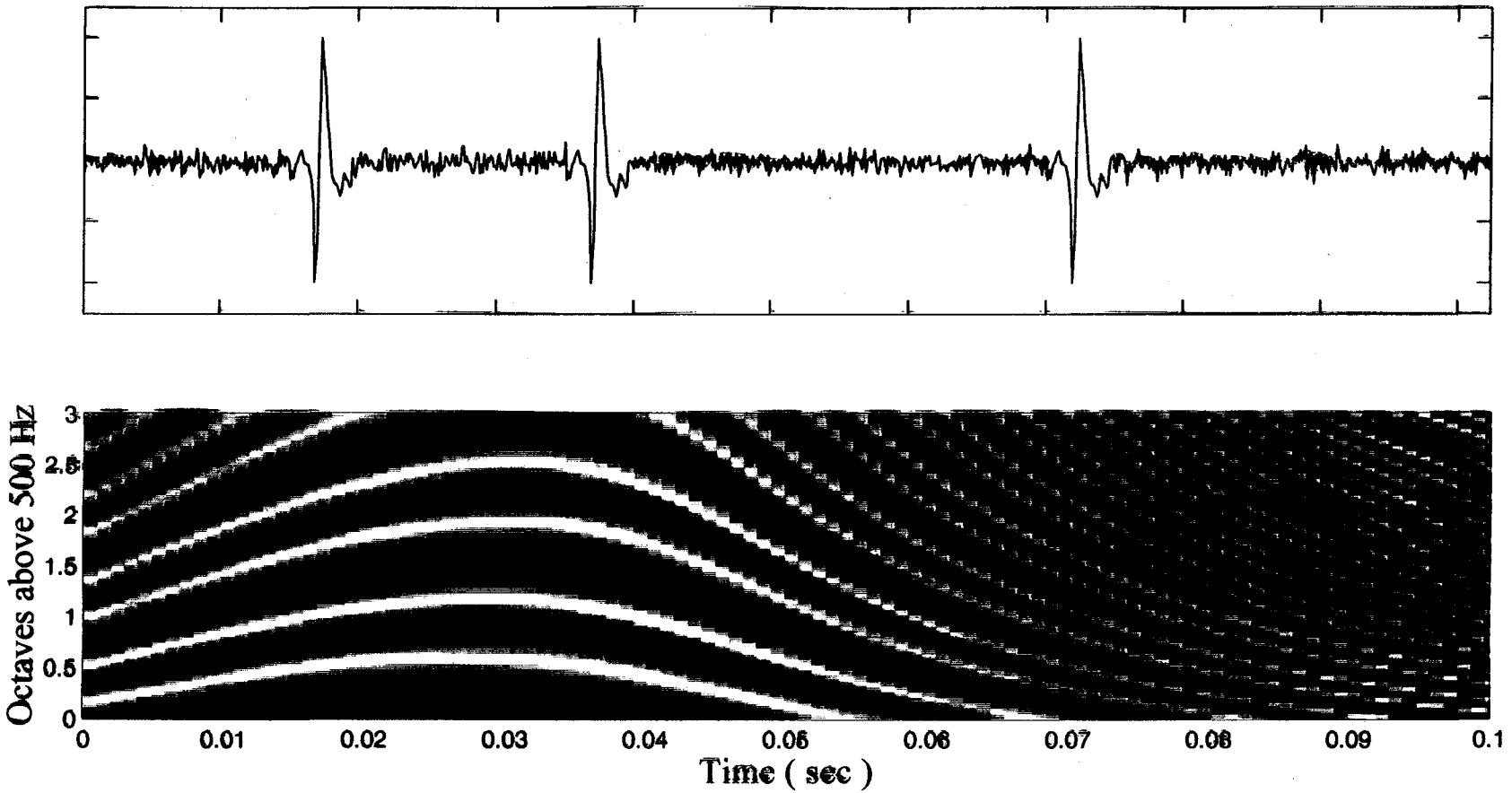

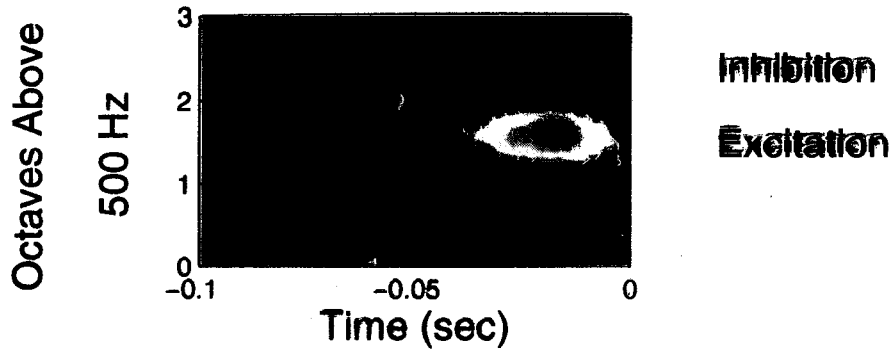

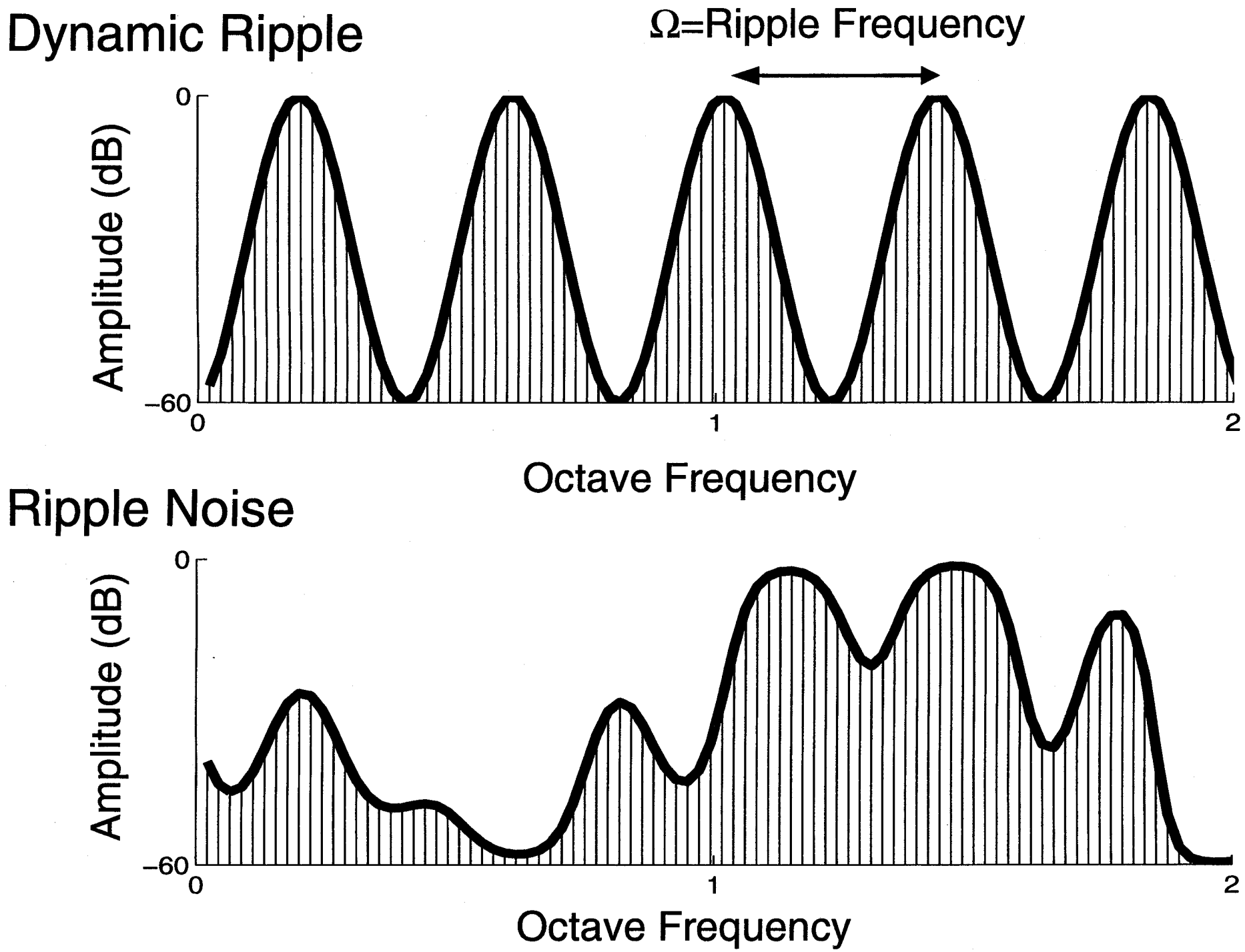
Dynamic Ripple
Ω=Ripple Frequency
Amplitude (dB)
0
–60
0
1
2
Octave Frequency
Ripple Noise
Amplitude (dB)
0
–60
0
1
2
Octave Frequency

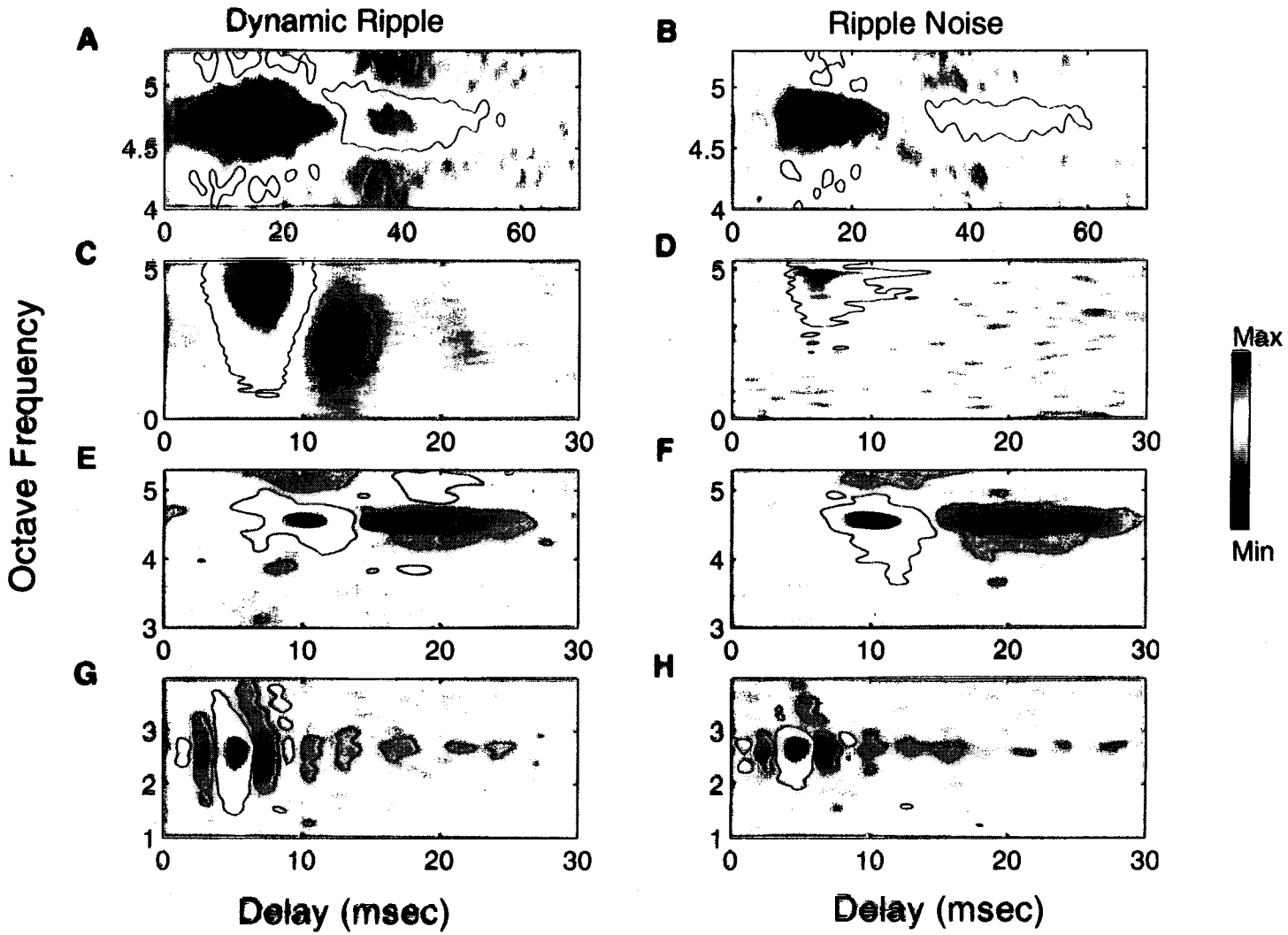
Dynamic Ripple
Ripple Noise
A
B
C
D
E
F
G
H
Octave Frequency
Delay (msec)
Delay (msec)
Max
Min

Feature Sensitive Cells

Moving Ripple STRF

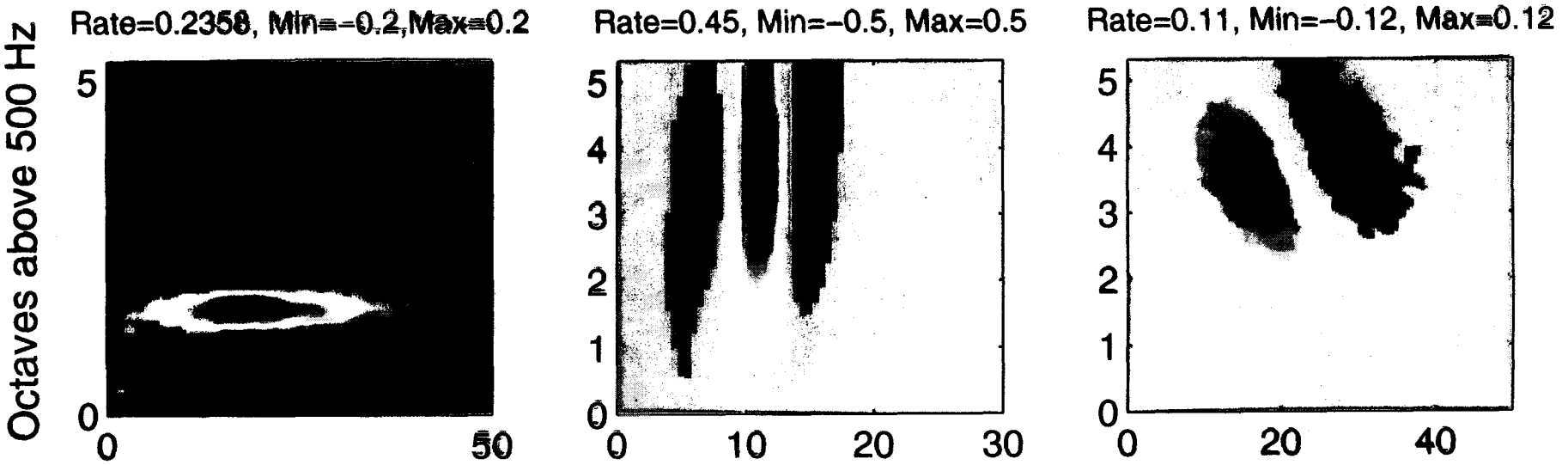

Ripple Noise STRF

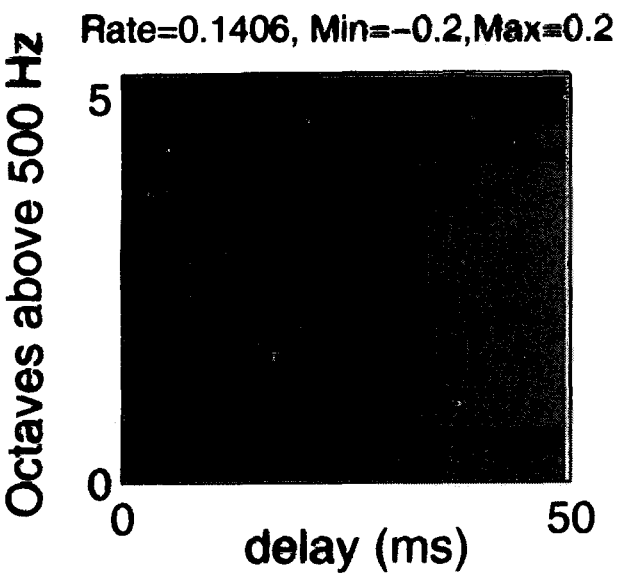

No Response

No Response

Complex Cells – Non Phase Locked

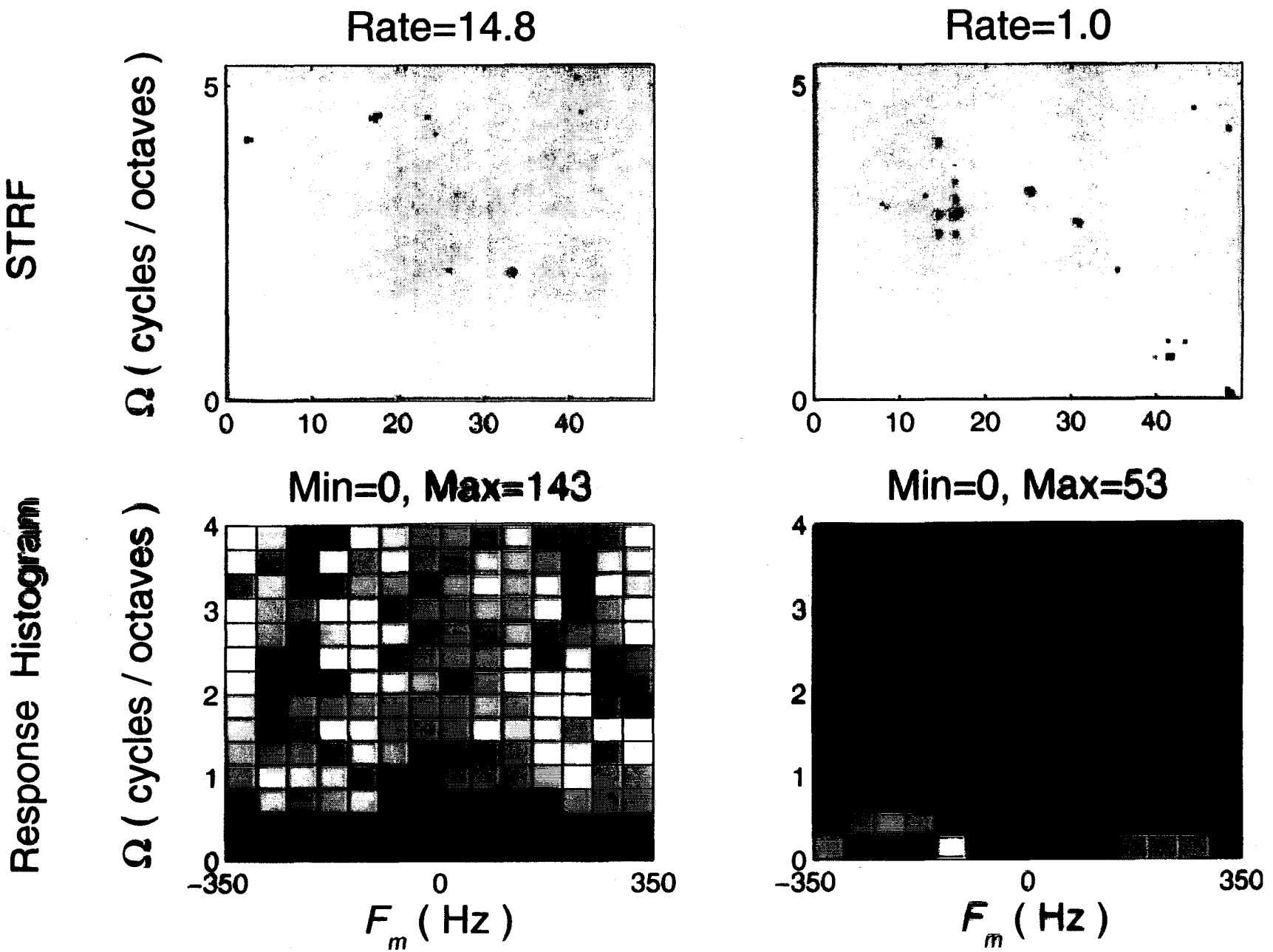

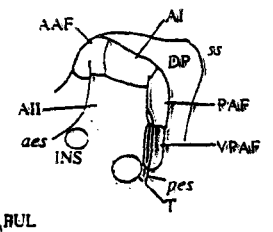

CORTEX

Tonotopic areas
(AAF, AI, PAF, VPAF)

Belt areas
(AII, T, INS, DP)

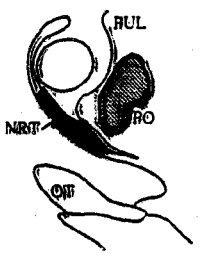

THALAMUS

Lateral part of the post. nucleus (PO)

Reticular nucleus (NRT)

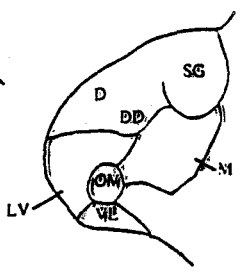

Medial geniculate body

Ventral division (LV, OV, VL)

Medial division (M)

Dorsal division (D, DD)

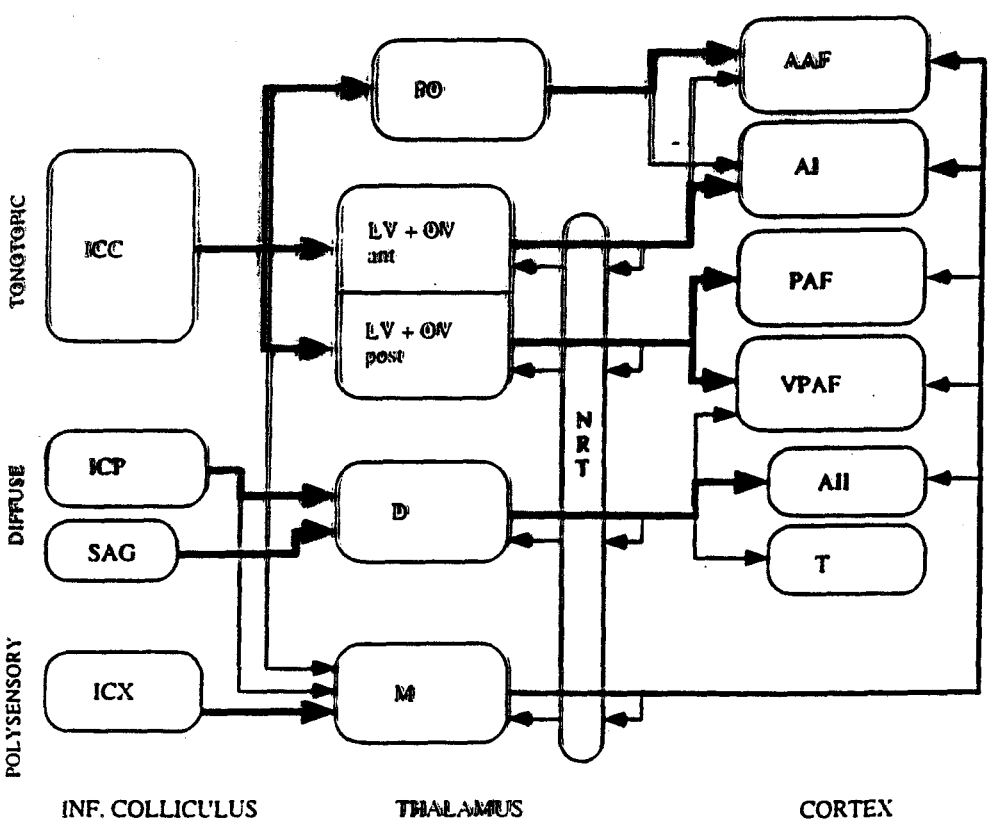

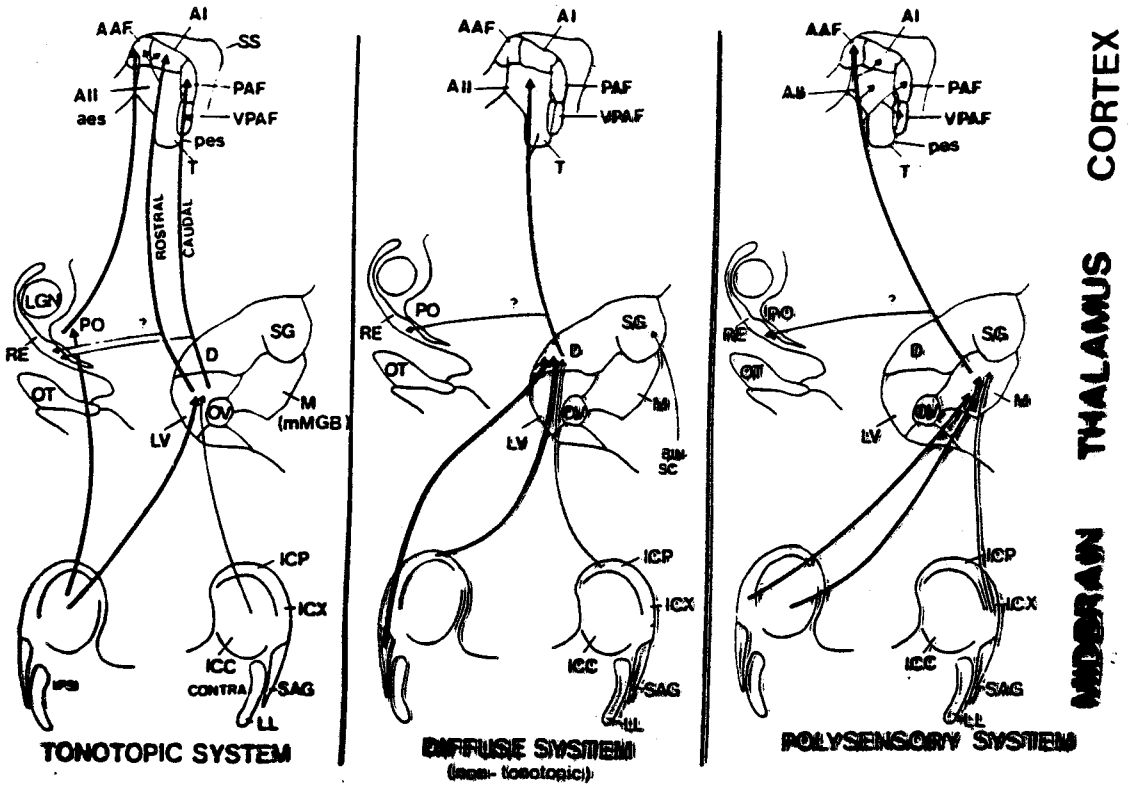
AAF
AI
SS
AII
aes
PAF
VPAF
pes
T
ROSTRAL
CAUDAL
LGN
PO
RE
D
SG
OT
OV
M
(mMGB)
LV
ICP
ICX
ICC
CONTRA
SAG
LL
TONOTOPIC SYSTEM
DIFFUSE SYSTEM
(non- tonotopic)
POLYSENSORY SYSTEM
CORTEX
THALAMUS
MIDBRAIN

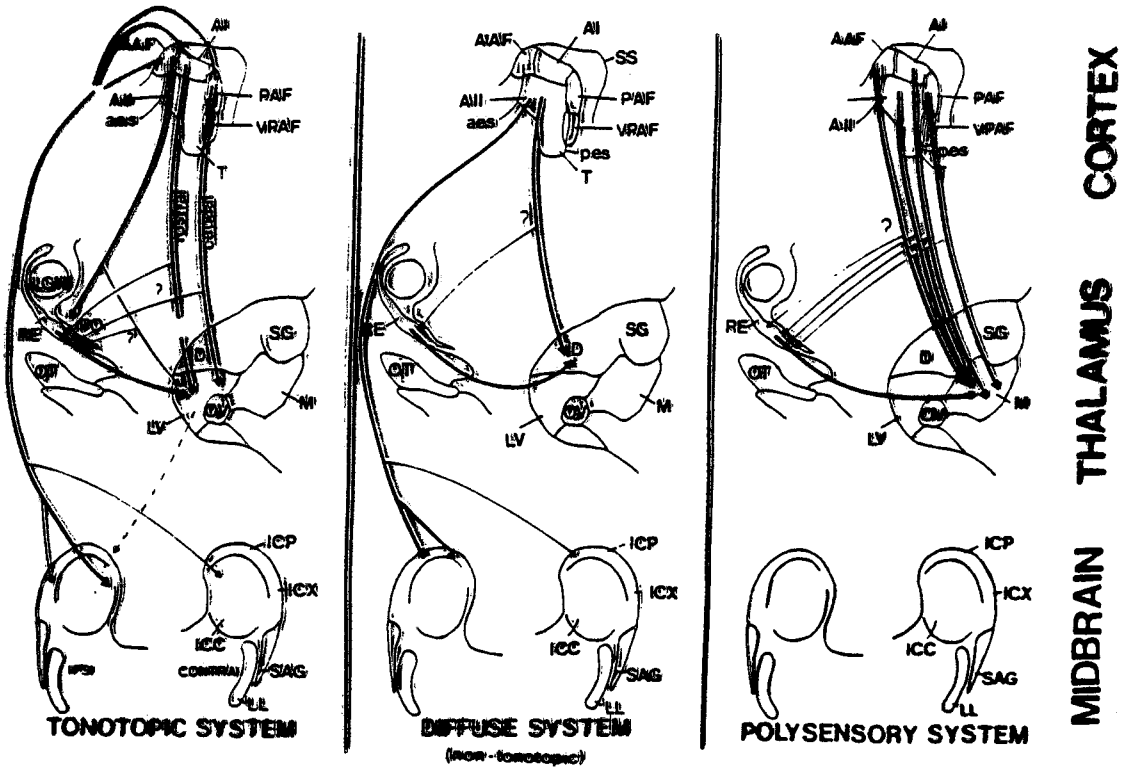
AAF
AI
SS
AII
aes
PAF
VPAF
pes
T
SG
D
M
LV
ICP
ICX
ICC
SAG
LL
TONOTOPIC SYSTEM
DIFFUSE SYSTEM
(non-tonotopic)
POLYSENSORY SYSTEM
CORTEX
THALAMUS
MIDBRAIN